Annu. Rev. Nucl. Part. Sci. 2004. 54:413–50
doi: 10.1146/annurev.nucl.54.070103.181302

GENERALIZED PARTON DISTRIBUTIONS

Xiangdong Ji
Department of Physics, University of Maryland, College Park, Maryland 20879; email: xji@physics.umd.edu

Key Words nucleon structure, quantum phase-space distributions, form factors, nucleon spin, quark orbital motion

PACS Codes 14.20.Dh, 12.38.−t, 13.40.−f

■ **Abstract** This review explains why generalized parton distributions and the related quantum phase-space distributions are useful in exploring the quark and gluon structure of the proton and neutron. It starts with the physics of form factors and parton distributions. Then quantum phase-space distributions and their offspring are discussed. The properties of generalized parton distributions are described. In particular, I elucidate the relation to the spin structure of the nucleon. Finally, various methods to determine the new distributions are explained.

CONTENTS

1. INTRODUCTION

In the past few years, generalized parton distributions (GPDs) have received considerable attention in both the theory and experimental communities. This article is an introduction to, but not a thorough review of, GPDs in hadrons (mostly the nucleon). The topics covered here were selected for their pedagogical utility. In particular, the material in the first two sections presents the view that quantum phase-space distributions are the fundamental physical observables, and GPDs are the observables needed to generate phase-space images of the quarks and gluons in hadrons. The discussion follows closely a recent paper by Belitsky, Yuan, and this author (1). For an up-to-date review of GPDs with many technical details and extensive references, the reader may consult Reference (2). Earlier views can be found in References (3–5), and some of the materials here overlap with those in Reference (3).

The subject of nucleon structure has been investigated extensively for several decades, so why do we care about another distribution? In understanding the microscopic structure of matter, we have so far relied mainly on two types of physical quantities. The first is the spatial distribution of matter (charge or current) in a system, which can be probed through elastic scattering of electrons, photons, neutrons, etc. The observables that one measures are the elastic form (structure) factors, which depend on three-momentum transfer to the system. The Fourier transformation of these form factors provides information about spatial distributions. The well-known examples include the charge distribution in an atom and the atomic structure of a crystal. The second type of quantity on which we rely is the distribution of constituents in momentum space, or simply the momentum distributions, which can be measured through deep-inelastic knockout scattering. The well-known examples contain the proton distribution in nuclei, measurable through quasielastic electron scattering, and the distribution of atoms in a quantum liquid probable through neutron scattering. With some modifications to accommodate the relativistic nature of the system, both experimental approaches have been used to explore the inside of the nucleon. The elastic nucleon form factors have been measured since the 1950s, and, at low-momentum transfer ($\ll$nucleon mass M_N) where the nucleon recoil effect is small, the three-dimensional Fourier transformation of the form factors is interpretable as the spatial charge and current distributions of quarks (6). On the other hand, Feynman parton distributions, measurable in high-energy hard collisions such as deep-inelastic scattering (DIS) and Drell-Yan and other hard processes, are the longitudinal-momentum distributions of the quarks and gluons in the so-called infinite momentum frame (7). Both observables have taught us a great deal about the nucleon, but they have similar deficiencies. The form factors contain no dynamical information on the constituents, such as

their speed and angular momentum, and the momentum distributions provide no knowledge of their spatial locations.

More complete information about the microscopic structure lies in the correlation between momentum and spatial coordinates, i.e., simultaneous knowledge of a contituent's location and velocity. This knowledge is certainly attainable for a classical system, for which one can define and study the phase-space distribution. For a quantum mechanical system, however, the notion of a phase-space distribution seems less useful because of the uncertainty principle: One cannot determine the position and conjugate momentum of a particle simultaneously. Nonetheless, the first quantum mechanical phase-space distribution was introduced by Wigner as early as 1932 (8), followed by many similar ones. These distributions have been used for various purposes in very diverse areas, such as heavy-ion collisions, quantum molecular dynamics, signal analysis, quantum information, optics, image processing, nonlinear dynamics, etc. (9). Thanks to the rapid experimental progress of the past decade, Wigner distributions (or functions) for many simple quantum systems are measurable (10–12), and provide remarkable insight about the dynamics of these systems.

The main question addressed in this article is, "Can one generalize the concept of phase-space distribution to the relativistic quarks and gluons in a hadron?" The notion of a correlated parton position-and-momentum distribution had not been systematically explored in quantum chromodynamics (QCD) until a few years ago. The relevant physical observable is GPDs. Roughly speaking, a GPD is a one-body matrix element that combines the kinematics of both elastic form factors and Feynman parton distributions, and is measurable in hard exclusive processes. GPDs were explicitly introduced in Reference (13) as objects with interesting perturbative QCD (pQCD) evolution, but were largely ignored because of unclear physical significance. They were rediscovered (14) in the study of quark orbital motion and the spin structure of the nucleon in which the physics potential of the distributions began to surface. In the past few years, a full picture of the role of GPDs in studying the quark and gluon structure of the nucleon has emerged. A crucial step has been the impact-parameter-space interpretation of GPDs at a particular kinematic point advocated by Burkardt (15). For a thorough list of references chronicling the rich and diverse development of the field, see Reference (2).

The organization of the article is as follows. Section 2 clarifies the effects of relativity on the physical interpretation of the form factors and parton distributions. Section 3 introduces quantum phase-space distributions and their offspring. I first summarize the main features of a quantum mechanical Wigner distribution, then introduce quantum phase-space parton distributions for a nucleon in its rest-frame, and finally relate them to experimental observables: transverse-momentum-dependent and generalized parton distributions. Section 4 reviews some general properties of the GPDs: their sum rules, relation to the spin structure of the nucleon, chiral behavior, partonic interpretation, scale evolutions, inequalities, and behaviors at large x and t. Section 5 discusses the GPD dynamics from various approaches: experimental measurements (hard exclusive processes such as deeply

virtual Compton scattering), lattice QCD calculations, and models and parameterizations. I present a model quantum phase-space distribution, illustrating what one might expect from future experimental data (1).

2. PHYSICS OF FORM FACTORS AND PARTON DISTRIBUTIONS

This section is devoted to the familiar topics of elastic form factors and Feynman parton distributions partly because a phase-space distribution or GPD is, in some sense, a hybrid of two basic observables. A more important reason, however, is that special relativity imposes strong constraints on the physical interpretations of these quantities. In fact, for nucleon physics, relativity is absolutely essential. In measuring the elastic form factors of the proton, the momentum transfer to the system can easily exceed the rest mass, resulting in a large Lorentz contraction in the recoil. In DIS, the struck quark travels along the light-cone: the world-line of an extreme relativistic particle. Clearly a proper exposition of the physics of form factors and momentum distributions in the relativistic domain is crucial to answering the question (1), "What sense does a phase-space quark distribution make?"

2.1. Form Factors and Scheme-Dependent Charge Distributions

The electromagnetic form factors are among the first measured and most studied observables of the nucleon (16). They are defined as the matrix elements of the electromagnetic current between the nucleon states of different four-momenta. Because the nucleon is a spin-1/2 particle, the matrix element defines two form factors,

$$\langle p_2|j_\mu(0)|p_1\rangle = \bar{U}(p_2)\left\{F_1(q^2)\gamma_\mu + F_2(q^2)\frac{i\sigma_{\mu\nu}q^\nu}{2M_N}\right\}U(p_1), \qquad 1.$$

where F_1 and F_2 are the well-known Dirac and Pauli form factors, respectively, depending on the momentum transfer $q = p_2 - p_1$ squared.

Since the 1950s, it has been known that the physical interpretation of the nucleon form factors is complicated by relativistic effects (17). Consider a system of size R and mass M. In relativistic quantum theory, the system cannot be localized to a precision better than its Compton wavelength $1/M$. Any attempt to do so with an external potential results in creation of particle-antiparticle pairs. As a consequence, the static size of the system cannot be defined to a precision better than $1/M$. Moreover, when the probing wavelength is comparable to $1/M$, its form factors are no longer determined by the internal structure alone. They contain, in addition, dynamical effects of the Lorentz boost to generate the final nucleon from the initial. Boost operators are interaction-dependent, and hence the nucleon wave function is different in different frames (in the usual instant form of quantization).

Therefore, in the region $|\vec{q}| \sim M$, the physical interpretation of the form factors is complicated by the entanglement of the internal and the center-of-mass motions. If $R \gg 1/M$, which is the case for nonrelativistic systems, relativity does not pose a significant constraint; one can probe the internal structure of the system with a wavelength $(1/|\vec{q}|)$ comparable to or even much smaller than R, but still large enough compared with $1/M$ so that the probe does not induce an appreciable recoil.

For the nucleon, $M_N R_N \sim 4$. Although much less certain than in the case of the hydrogen atom, it is still sensible to have a rest-frame picture in terms of the electromagnetic form factors, so long as one keeps in mind that equally justified definitions of the nucleon size can differ by $\sim 1/M_N(R_N M_N)$. For example, the traditional definition of the proton charge radius in terms of the slope of the Sachs form factor $G_E(q^2)$ is 0.86 fm. On the other hand, if one uses the slope of the Dirac form factor F_1 to define the charge radius, one gets 0.79 fm, about 10% smaller. The form factors at $|\vec{q}| \geq M_N \sim 1$ GeV definitely cannot be interpreted as information about the internal structure alone.

Because relativity makes the interpretation of the electromagnetic form factors nonunique, the best one can do is to choose an interpretation and work with it consistently. For example, when extracting the proton charge radius from the Lamb shift measurements, one should use the same definition as that from the electric form factor. The most frequently used form-factor interpretation is that of Sachs (6), but other schemes are equally good and the scheme dependence disappears in the limit $MR \to \infty$. This is very much like the renormalization scheme dependence of parton densities due to radiative corrections at a finite coupling constant α_s. Although the $\overline{\text{MS}}$ scheme is the most popular in the literature, one can define the parton densities in any other scheme to correlate physical observables.

In this article, I adopt the Sachs interpretation of the form factors. To appreciate the motivation for this scheme, let us review the argument offered by Sachs et al. (6). To establish the notion of a static (charge) distribution, one must create a wave packet representing a proton localized at $\vec{R}$

$$|\vec{R}\rangle = \int \frac{d^3\vec{p}}{(2\pi)^3}\, e^{i\vec{p}\cdot\vec{R}}\, \Psi(\vec{p})|\vec{p}\rangle, \qquad 2.$$

where the plane-wave state $|\vec{p}\rangle$ is normalized in a relativistic-covariant manner, $\langle\vec{p}_2|\vec{p}_1\rangle = 2E_{\vec{p}_1}(2\pi)^3\delta^{(3)}(\vec{p}_1 - \vec{p}_2)$. With the above, we can calculate, for example, the charge distribution relative to the center of the wave packet, $\rho(\vec{r}) = \langle\vec{R} = 0|\, j_0(\vec{r})|\vec{R} = 0\rangle$, where $\vec{r}$ measures the relative distance to the center $\vec{R} = 0$. Taking its Fourier transform, one gets

$$\begin{aligned} F(\vec{q}) &\equiv \int d^3\vec{r}\, e^{i\vec{q}\cdot\vec{r}}\rho(\vec{r}) \\ &= \int \frac{d^3\vec{p}}{(2\pi)^3}\Psi^*\left(\vec{p} + \vec{q}/2\right)\Psi\left(\vec{p} - \vec{q}/2\right)\langle\vec{p} + \vec{q}/2|\, j_0(0)\,|\vec{p} - \vec{q}/2\rangle, \qquad 3. \end{aligned}$$

where we have changed the momentum integration variables, with $\vec{p}$ representing the average momentum of the initial and final protons. It is important to point out that the resolution momentum $\vec{q}$ is now linked to the difference in the initial- and final-state momenta. In nonrelativistic quantum systems, because of the large masses, the momentum transfer causes little change in velocity, and hence the initial and final states have practically the same intrinsic wave functions.

To remove the effects of the wave packet, the necessary condition on $\Psi(\vec{p})$ is that the coordinate-space size of the wave packet must be much smaller than the system size $|\delta\vec{r}| \ll R_N$. Furthermore, the probing wavelength, or resolution scale, must also be large compared to the size of the wave packet $1/\vec{q} \gg \delta\vec{r} \sim 1/\vec{p}$. Then one can ignore $\vec{q}$-dependence in Ψ, so that $\Psi(\vec{p} \pm \frac{1}{2}\vec{q}) \approx \Psi(\vec{p})$

$$F(\vec{q}) = \int \frac{d^3\vec{p}}{(2\pi)^3} |\Psi(\vec{p})|^2 \langle \vec{p} + \vec{q}/2|\, j_0(0)\, |\vec{p} - \vec{q}/2\rangle\,. \qquad 4.$$

On the other hand, to be insensitive to the antiparticle degrees of freedom, the wave packet must be larger than the proton Compton wavelength $|\delta\vec{r}| \gg 1/M_N$. In the momentum space, this corresponds to a restriction on momenta allowed in the wave packet, $|\vec{p}| \ll M_N$. Therefore the combined constraint on the wave packet profile is $1/R_N \ll |\vec{q}| \ll |\vec{p}| \ll M_N$. The extreme limit of the last inequality yields a wave packet with a zero-momentum nucleon, $|\Psi(\vec{p})|^2 = \frac{(2\pi)^3}{2M_N}\delta^{(3)}(\vec{p})$, which gives

$$2M_N F(\vec{q}) = \langle \vec{q}/2|\, j_0(0)\, |-\vec{q}/2\rangle\,. \qquad 5.$$

This is the matrix element of the charge density in the Breit frame, and is $2M_N G_E(t) w_2^* w_1$, where $G_E(t) = F_1(t) + \frac{t}{4M_N^2} F_2(t)$ is the Sachs electric form factor ($t = -\vec{q}^2$). Hence, G_E is a Fourier transformation of the proton charge distribution. Similar analysis finds $G_M(t) = F_1(t) + F(t)$ as the Fourier transformation of the magnetization density.

2.2. Physics of Parton Distributions in the Rest Frame

Parton distributions were introduced by Feynman to describe DIS (7). They have the simplest interpretation in the infinite momentum frame as the densities of partons in the longitudinal momentum x. In QCD, the quark distribution is defined through the following matrix element:

$$q(x) = \frac{1}{2p^+} \int \frac{d\lambda}{2\pi} e^{i\lambda x} \langle p|\bar{\Psi}(0)\gamma^+ \Psi(\lambda n)|p\rangle. \qquad 6.$$

Equation 6 uses the standard light-cone notation $p^\pm = (p^0 \pm p^3)/\sqrt{2}$. The vector n^μ is along the direction of $(1, 0, 0, -1)$, and $n \cdot p = 1$. The notation Ψ is a quark field with an associated gauge link that extends from the position of the quark to infinity along the light-cone n^μ, and hence is gauge-invariant in nonsingular gauges. The renormalization scale dependence is implicit. In light-cone quantization (18),

it is easy to show

$$q(x)|_{x>0} = \frac{1}{2x}\sum_{\lambda=\uparrow\downarrow}\int\frac{d^2\vec{k}_\perp}{(2\pi)^3}\frac{\langle p|b_\lambda^\dagger(k^+,\vec{k}_\perp)b_\lambda(k^+,\vec{k}_\perp)|p\rangle}{\langle p|p\rangle},$$

$$q(x)|_{x<0} = \frac{-1}{2x}\sum_{\lambda=\uparrow\downarrow}\int\frac{d^2\vec{k}_\perp}{(2\pi)^3}\frac{\langle p|d_\lambda^\dagger(k^+,\vec{k}_\perp)d_\lambda(k^+,\vec{k}_\perp)|p\rangle}{\langle p|p\rangle}, \qquad 7.$$

where $b^\dagger$ and $d^\dagger$ are creation operators of a quark and an antiquark, respectively, with longitudinal momentum $k^+ \equiv xp^+$ and transverse momentum $\vec{k}_\perp$. The interpretation as parton densities is then obvious.

To construct a quantum phase-space distribution, we need an interpretation of the Feynman distribution in the rest frame. This is because the infinite momentum frame involves a Lorentz boost along the z direction, introducing a Lorentz contraction on a three-dimensional system, which we try to avoid here. However, if one works in the rest frame, the two quark fields in Equation 6 are no longer simultaneous. If one Fourier-expands one of the fields in terms of quark creation and annihilation operators, the other must be determined from the Heisenberg equation of motion. The result is that the bilinear quark operator takes a very complicated expression in terms of the creation and annihilation operators in equal-time quantization.

The rest-frame physics of Feynman distributions is made clear through the "spectral function,"

$$S(k) = \frac{1}{2p^+}\int d^4\xi e^{ik\cdot\xi}\langle p|\bar{\Psi}(0)\gamma^+\Psi(\xi)|p\rangle, \qquad 8.$$

which is the dispersive part of a single-quark Green's function in the nucleon. The physical meaning of $S(k)$ can be seen from its spectral representation,

$$\begin{aligned} S(k) &= \sum_n (2\pi)^4\delta^{(4)}(p-k-p_n)\langle p|\bar{\Psi}_k|n\rangle\gamma^+\langle n|\Psi(0)|p\rangle/2p^+ \\ &\sim \sum_n (2\pi)^4\delta^{(4)}(p-k-p_n)|\langle n|\Psi_{k+}|p\rangle|^2, \end{aligned} \qquad 9.$$

where Ψ_k is a Fourier transformation of $\Psi(\xi)$: It is the probability of annihilating a quark (or creating an antiquark) of four-momentum k (three-momentum $\vec{k}$ and the off-shell energy $E = k^0$) in the nucleon, leading to an "on-shell" state of energy-momentum $p_n = p - k$. The quark here is off-shell because if p_n and p are both "on-shell," $k^2 \neq m_q^2$ in general. (That the partons are off-shell is in fact also true in infinite-momentum-frame calculations.) Of course, in QCD $|n\rangle$ is not in the Hilbert space, but the spectral function itself is still a meaningful physical quantity.

Because the quarks are ultrarelativistic, Ψ_k contains both quark and antiquark Fock operators. One cannot in general separate quark and antiquark contributions, unlike in the nonrelativistic systems, in which only the particle or antiparticle

contributes. In fact, if one expands the above expression, one finds pair creations and annihilation terms. This is also true for the charge density discussed in the previous subsection. Therefore, we can only speak of $S(k)$ as a distribution of charges and currents, not as a "particle density." In nuclear physics, where the nonrelativistic dynamics dominates, the nucleon spectral function in a nucleus is positive-definite and can be regarded as a particle density. The function is directly measurable through pickup and knockout experiments, in which E and $\vec{k}$ are called the missing energy and missing momentum, respectively (see, e.g., Reference (19)).

It is now easy to see that in the rest frame of the proton, the Feynman quark distribution is

$$q(x) = \sqrt{2} \int \frac{d^4k}{(2\pi)^4} \delta\big(k^0 + k^z - xM_N\big) S(k). \qquad 10.$$

The x variable is simply a special combination of the off-shell energy $k^0 = E$ and momentum component k^z. The parton distribution is the spectral function of quarks projected along a special direction in the four-dimensional energy-momentum space. The quarks with different E and k^z may have the same x, and moreover, both the $x > 0$ and $x < 0$ distributions contain contributions from quarks and antiquarks.

To summarize, in the nucleon rest frame, the quarks are naturally off-shell and hence have a distribution in the four-dimensional energy-momentum space. The Feynman distribution results from a reduction of the spectral function in the momentum space orthogonal to the $k^z + E$ direction.

3. QUANTUM PHASE-SPACE DISTRIBUTIONS AND THEIR OFFSPRING

Having established the concept of phase-space distribution in nonrelativistic quantum mechanics, I generalize it in this section to relativistic quantum field theories—in particular, to quarks and gluons in QCD. The procedure is not unique; however, we are guided by the requirement that the resulting distributions must be experimental observables.

In classical physics, the state of a particle is specified by its position $\vec{r}$ and momentum $\vec{p}$. In a gas of classical particles, the single-particle properties are described by a phase-space distribution $f(\vec{r}, \vec{p})$ that represents the density of particles at a phase-space point $(\vec{r}, \vec{p})$. The time evolution of the distribution is governed by the Boltzmann equation, or by the Liouville equation if the particles are not interacting. In quantum mechanics, position and momentum operators do not commute and hence, in principle, one cannot entertain a joint momentum and position distribution of particles. Indeed, the quantum mechanical wave functions depend on either spatial coordinates or momentum but not both. Nonetheless, Wigner introduced the first quantum phase-space distribution just a few years after quantum

mechanics was formulated (8). It is not positive-definite and hence cannot be regarded as a probability distribution. However, it reduces to the positive-definite classical phase-space distribution in the $\hbar \to 0$ limit. The sign oscillation in the phase-space is essential to reproduce quantum interference effects. The Wigner distribution contains the complete single-particle information about a quantum system (equivalent to the full single-particle density matrix) and can be used to calculate any single-particle observable through classical-type phase-space averages.

3.1. A Brief Introduction to Wigner Distribution

There is a vast literature on quantum phase-space distributions and the Wigner distribution in particular. This subsection summarizes some salient features.

Suppose we have a one-dimensional quantum mechanical system with wave function $\psi(x)$. The Wigner function or distribution is defined as

$$W(x, p) = \int d\eta e^{ip\eta} \psi^*(x - \eta/2)\psi(x + \eta/2), \qquad 11.$$

where we have set $\hbar = 1$. When integrating out the coordinate x, one gets the momentum density $|\psi(p)|^2$, which is positive-definite. When integrating out p, the positive-definite coordinate space density $|\psi(x)|^2$ follows. For arbitrary p and x, the Wigner distribution is not positive-definite and does not have a probability interpretation. Nonetheless, to calculate the physical observables, one simply takes averages over the phase-space as if it were a classical distribution,

$$\langle \hat{O}(x, p) \rangle = \int dx\, dp\, W(x, p) O(x, p), \qquad 12.$$

where the operators are ordered according to the Weyl association rule. For a single-particle system, the Wigner distribution contains everything there is in the quantum wave function. For a many-body system, the distribution can be used to calculate the averages of all one-body operators.

In the classical limit, the Wigner distribution is expected to become classical phase-space distribution. For systems that are statistical ensembles, the limit $\hbar \to 0$ is often well-behaved. For example, for an ensemble of harmonic oscillators at finite temperature, the Wigner distribution becomes the classical Boltzmann distribution as $\hbar \to 0$ (see, e.g., Reference (20)). The Wigner distribution for the nth excited state of the one-dimensional harmonic oscillator of energy $E_n = \hbar\omega(n + \frac{1}{2})$ is (21)

$$W_n(p, x) = \frac{(-1)^n}{\pi\hbar} e^{-2H/(\hbar\omega)} L_n\left(\frac{4H}{\hbar\omega}\right), \qquad 13.$$

where H stands for the hamiltonian $H(p, x) = p^2/(2m) + m\omega^2 x^2/2$ and L_n is the nth Laguerre polynomial. In the quasiclassical limit—vanishing Planck constant and large quantum numbers—the oscillator Wigner distribution turns into the generalized distribution residing on the classical trajectories $E_\infty =$ fixed,

$$\lim_{\hbar\to 0,\, n\to\infty} W_n(p,x) \sim \delta(H(p,x) - E_\infty). \qquad 14.$$

Phase-space averaging with this kernel is equivalent to calculating observables using the classical equations of motion. This can be easily understood from the semiclassical form of the wave function,

$$\psi(x) = C(x)\mathrm{e}^{iS(x)/\hbar}. \qquad 15.$$

Substituting this into Equation 11 and expanding S to the first order in $\hbar$, one gets the quasiclassical Wigner distribution,

$$W(p,x) = |C|^2\delta\left(p - \frac{\partial S(x)}{\partial x}\right), \qquad 16.$$

where the argument of the δ-function describes a family of classical paths.

The quantum mechanical Wigner distribution is measurable. The actual measurement has been performed for a very simple quantum system—the quantum state of a light mode (a pulse of laser light of given frequency)—employing the ideas of Vogel & Risken (10). It was extracted via the method of homodyne tomography (11) by measurement of a marginal observable and subsequent reconstruction by inverse Radon transformation. Recently this Wigner distribution was measured directly by means of the photon counting techniques based on a Mach-Zender interferometric scheme (12).

Other versions of phase-space distributions are possible. They are all members of the "Cohen class" (22), of which Husimi and Kirkwood distributions (23) are the best-known representatives. The Husimi distribution is a smeared version of the Wigner distribution defined by projection of the wave function on the coherent state (Gaussian wave packet)

$$H(\bar{p},\bar{x}) = \int dp'dx'\, W(p',x')W_{\mathrm{coh}}(p'-\bar{p},x'-\bar{x}),$$

which is real and positive-definite. In contrast, the Kirkwood function is complex. Once again, all these distributions are expected to reduce to the same phase-space distribution in the $\hbar \to 0$ limit.

3.2. Quantum Phase-Space Parton Distributions

Let us generalize phase-space distribution to relativistic quarks and gluons in the nucleon (24). The single-particle wave function is replaced by a quantum field in quantum field theory, and hence it is natural to introduce the "Wigner operator,"

$$\widehat{\mathcal{W}}_\Gamma(\vec{r},k) = \int d^4\eta \mathrm{e}^{ik\cdot\eta}\bar{\Psi}(\vec{r}-\eta/2)\Gamma\Psi(\vec{r}+\eta/2), \qquad 17.$$

where $\vec{r}$ is the quark phase-space position and k the phase-space four-momentum conjugated to the space-time separation η. The matrix Γ is a Dirac matrix that defines the types of quark distributions because the quarks are spin-1/2 relativistic

particles. Depending on the choice of Γ, we have vector, axial vector, or tensor Wigner operators.

Because QCD is a gauge theory, the product of two quark fields at different space-time points is not automatically gauge-invariant. One can define a gauge-invariant quark field by adding a gauge link to the space-time infinity along a constant four-vector ζ^μ,

$$\Psi(\eta) = \exp\left(-ig\int_0^\infty d\lambda\,\zeta\cdot A(\lambda\zeta+\eta)\right)\psi(\eta), \qquad 18.$$

where we choose a nonsingular gauge in which the gauge potential vanishes at the space-time infinity (25–27). Although gauge-invariant, the Wigner operator depends on the choice of ζ^μ. Although theoretically any ζ^μ is possible, it is constrained, in real observables, to be the light-cone vector n^μ by the experimental probes.

The Wigner distribution has been extended to include the time variable. Therefore, besides the dependence on the three-momentum, there is also a dependence on the energy. For the bound states in a simple system, such as those in a simple harmonic oscillator, the energy dependence is a δ-function that singles out the binding energies. For many-body systems, however, the energy dependence is more complicated, as it reflects the energy distribution of the resulting states after one particle is removed from the system.

For nonrelativistic systems for which the center of mass is well-defined and fixed, one can define phase-space distributions by taking the expectation value of the above Wigner operators in the center-of-mass $\vec{R}=0$ state. For the proton, for which the recoil effects cannot be neglected, the rest-frame state cannot be uniquely defined, as elaborated in Section 2. Here we follow Sachs, constructing a "rest-frame" matrix element actually in the Breit frame, followed by averaging over all possible three-momentum transfers. Therefore, we define quantum phase-space quark distribution in the nucleon as

$$\begin{aligned} W_\Gamma(\vec{r},k) &= \frac{1}{2}\int\frac{d^3\vec{q}}{(2\pi)^3}\langle\vec{q}/2|\widehat{\mathcal{W}}_\Gamma(\vec{r},k)|-\vec{q}/2\rangle \\ &= \frac{1}{2}\int\frac{d^3\vec{q}}{(2\pi)^3}e^{-i\vec{q}\cdot\vec{r}}\langle\vec{q}/2|\widehat{\mathcal{W}}_\Gamma(0,k)|-\vec{q}/2\rangle, \end{aligned} \qquad 19.$$

where the plane-wave states are normalized relativistically. The most general phase-space distribution depends on seven independent variables. However, there is no known experiment that measures this function.

The only way we know how to probe the single-particle distributions is through high-energy processes, in which the light-cone energy $k^- = (k^0-k^z)/\sqrt{2}$ is difficult to measure (the z-axis refers to the momentum transfer direction of a probe). Moreover, the leading observables in these processes are associated with the "good" components of the quark (gluon) fields in the sense of light-cone quantization (18),

which can be selected by $\Gamma = \gamma^+$, $\gamma^+\gamma_5$, or $\sigma^{+\perp}$, where $\gamma^+ = (\gamma^0 + \gamma^z)/\sqrt{2}$. The direction of the gauge link, ζ^μ, is then determined by the trajectories of high-energy partons traveling along the (near) light-cone $n = (1, 0, 0, -1)$ (27, 30). Therefore, from now on, we restrict ourselves to the reduced Wigner distributions by integrating out k^-,

$$W_\Gamma(\vec{r}, \vec{k}) = \int \frac{dk^-}{(2\pi)^2} W_\Gamma(\vec{r}, k), \qquad 20.$$

with a light-cone gauge link implied. However, no known experiment can measure this six-dimensional distribution either.

3.3. Transverse-Momentum-Dependent Parton Distributions

Integrating over $\vec{r}$ in Equation 20, we obtain the transverse-momentum-dependent (TMD) parton distributions. For $\Gamma = \gamma^+$,

$$\int \frac{d^3\vec{r}}{(2\pi)^2} W_{\gamma^+}(\vec{r}, \vec{k}) = q(x, k_\perp) + q_T(x, k_\perp)(\hat{k}_\perp \times \hat{S}_\perp) \cdot \hat{P}$$

$$= \frac{1}{2} \int \frac{d^2\eta_\perp d\eta^-}{(2\pi)^3} e^{i(k^+\xi^- - \vec{k}_\perp \cdot \vec{\eta}_\perp)} \langle P|\bar{\Psi}(0)\gamma^+\Psi(\eta^-, \vec{\eta}_\perp)|P\rangle. \qquad 21.$$

The new distributions generalize those of Feynman with additional information about partons' transverse momentum. For example, $q(x, \vec{k}_\perp)$ is, roughly speaking, the probability of finding a quark with longitudinal momentum $x P^+$ and transverse momentum $\vec{k}_\perp$ in a nucleon (or hadron) with four-momentum $P^\mu = (P^0, 0, 0, P^3)$.

The transverse-polarization $\hat{S}_\perp$-dependent term $q_T(x, k_\perp)$ was first introduced by Sivers and has been called the Sivers function in the literature (28). Physically, it signifies that the parton momentum distribution in a transversely polarized nucleon is not rotationally invariant along the z direction—it has an azimuthal dependence. The term violates the naive time-reversal invariance; however, a careful examination indicates that time reversal does not forbid its existence because the quark field Ψ contains the guage link. It has been shown phenomenologically that $q_T(x, k_\perp)$ can be responsible for the target single-spin asymmetry observed in semi-inclusive deep-inelastic production of pions (29, 30).

Boer, Mulders, and Tangerman systematically classified all the leading-twist TMD parton distributions (31, 32). When $\Gamma = \gamma^+\gamma_5$, one finds

$$\int \frac{d^3\vec{r}}{(2\pi)^2} W_{\gamma^+\gamma_5}(\vec{r}, \vec{k}) = \Delta q_L(x, k_\perp)(S \cdot n) + \Delta q_T(x, k_\perp)(\hat{k}_\perp \cdot \hat{S}_\perp)$$

$$= \frac{1}{2} \int \frac{d^2\eta_\perp d\eta^-}{(2\pi)^3} e^{i(k^+\eta^- - \vec{k}_\perp \cdot \vec{\eta}_\perp)} \langle P|\bar{\Psi}(0)\gamma^+\gamma_5\Psi(\eta^-, \vec{\eta}_\perp)|P\rangle, \qquad 22.$$

where $\Delta q_T(x, k_\perp)$ is a novel quark helicity distribution in a transversely polarized nucleon. With $\Gamma = \sigma^{+\perp}\gamma_5$, one has four TMD distributions,

$$\int \frac{d^3\vec{r}}{(2\pi)^2} W_{\sigma^{+\perp}\gamma_5}(\vec{r}, \vec{k})$$
$$= \delta q_T(x, k_\perp)\hat{S}_T + \delta q_{T'}(x, k_\perp)\hat{k}_\perp(\hat{k}_\perp \cdot \hat{S}_\perp) + \delta q_L(x, k_\perp)\hat{k}_\perp(S \cdot n) + \delta q(x, k_\perp)\hat{k}_\perp$$
$$= \frac{1}{2}\int \frac{d^2\eta_\perp d\eta^-}{(2\pi)^3} e^{i(k^+\eta^- - \vec{k}_\perp\cdot\vec{\eta}_\perp)}\langle P|\bar{\Psi}(0)\sigma^{+\perp}\gamma_5\Psi(\eta^-, \eta_\perp)|P\rangle, \quad 23.$$

where $\delta q(x, k_\perp)$ is a transversity distribution in an unpolarized nucleon and vanishes under naive time-reversal transformation; $\delta q_L(x, k_\perp)$ is a transversity distribution in a longitudinally polarized nucleon.

TMD distributions have wide-ranging phenomenological applications in semi-inclusive DIS, the Drell-Yan process, and back-to-back jet production in e^+e^- annihilation (31–33). Without going into the details here, I offer a couple of theoretical comments:

First, physical interpretation and gauge invariance of these new distributions are subtle. Usually, the parton distributions are simplest to interpret in the light-cone gauge $A^+ = 0$, in which the light-cone gauge link vanishes. However, it turns out that the above definition is good only in nonsingular gauges. In the light-cone gauge, we must introduce additional gauge links at infinity to make the distribution gauge-invariant (27, 34). When we do so, however, a straightforward parton interpretation is no longer possible.

Second, unlike the usual parton distribution, TMD distributions are sensitive to the rapidity cutoff of the partons. Without such a cutoff, there is a light-cone divergence (see, e.g., Reference (35) and references therein). The rapidity cutoff is in general not commutable with the transverse momentum integration. As a consequence, for a regularized TMD parton distribution, even when $k_\perp$ is integrated, the distribution does not simply go back to an integrated parton distribution.

3.4. Generalized Parton Distributions and Phase-Space Quark Images

An alternative way of reducing $W_\Gamma(\vec{r}, \vec{k})$ is to integrate out the transverse momentum of the quarks. We then have a four-dimensional quantum distribution,

$$\tilde{f}_\Gamma(\vec{r}, k^+) = \int \frac{d^2\vec{k}_\perp}{(2\pi)^2} W_\Gamma(\vec{r}, \vec{k})$$
$$= \frac{1}{2}\int \frac{d^3\vec{q}}{(2\pi)^3} \mathrm{e}^{-i\vec{q}\cdot\vec{r}} \int \frac{d\eta^-}{2\pi} \mathrm{e}^{i\eta^- k^+}$$
$$\times \langle \vec{q}/2|\bar{\Psi}(-\eta^-/2)\Gamma\Psi(\eta^-/2)|-\vec{q}/2\rangle. \quad 24.$$

As we shall see, the matrix element under the momentum integral defines the GPDs. Indeed, if one replaces k^+ by Feynman variable xp^+ (with $p^+ = E_q/\sqrt{2}$, proton energy $E_q = \sqrt{M^2 + \vec{q}^2/4}$) and η^- by λ/p^+, the above distribution becomes

$$f_\Gamma(\vec{r}, x) = \int \frac{d^3\vec{q}}{(2\pi)^3} e^{-i\vec{q}\cdot\vec{r}} F_\Gamma(x, \xi, t). \qquad 25.$$

In this equation, $\xi = q^z/(2E_q)$, $t = -\vec{q}^2$, and

$$F_\Gamma(x, \xi, t) = \frac{1}{2p^+} \int \frac{d\lambda}{2\pi} e^{i\lambda x} \langle \vec{q}/2|\bar{\Psi}(-\lambda n/2)\Gamma\Psi(\lambda n/2)| - \vec{q}/2\rangle, \qquad 26.$$

which generates the leading-twist GPDs for different choices of Γ.

Taking $\Gamma = \gamma^+$, we write (14)

$$\begin{aligned} F_{\gamma^+}(x, \xi, t) &= \frac{1}{2p^+} \int \frac{d\lambda}{2\pi} e^{i\lambda x} \langle \vec{q}/2|\bar{\Psi}(-\lambda n/2)\gamma^+\Psi(\lambda n/2)| - \vec{q}/2\rangle \\ &= \frac{1}{2p^+} \bar{U}(\vec{q}/2) \left[H(x, \xi, t)\gamma^+ + E(x, \xi, t)\frac{i\sigma^{+i}q_i}{2M} \right] U(-\vec{q}/2), \end{aligned} \qquad 27.$$

where $H(x, \xi, t)$ and $E(x, \xi, t)$ are the two GPDs. On the other hand, if one takes $\Gamma = \gamma^+\gamma_5$, then

$$\begin{aligned} F_{\gamma^+\gamma_5}(x, \xi, t) &= \frac{1}{2p^+} \int \frac{d\lambda}{2\pi} e^{i\lambda x} \langle \vec{q}/2|\bar{\Psi}(-\lambda n/2)\gamma^+\gamma_5\Psi(\lambda n/2)| - \vec{q}/2\rangle \qquad 28. \\ &= \frac{1}{2p^+} \bar{U}(\vec{q}/2) \left[\tilde{H}(x, \xi, t)\gamma^+ + \tilde{E}(x, \xi, t)\frac{i\sigma^{+i}q_i}{2M} \right] U(-\vec{q}/2), \end{aligned}$$

which defines two more GPDs. Finally, if one chooses $\Gamma = \sigma^{+\perp}\gamma_5$, then (36, 37)

$$\begin{aligned} F_{\sigma^{+i}\gamma_5}(x, \xi, t) &= \frac{1}{2p^+} \int \frac{d\lambda}{2\pi} e^{i\lambda x} \langle \vec{q}/2|\bar{\Psi}(-\lambda n/2)\sigma^{+i}\gamma_5\Psi(\lambda n/2)| - \vec{q}/2\rangle \qquad 29. \\ &= \frac{1}{2p^+} \bar{U}(\vec{q}/2) \left[H_T(x, \xi, t)\gamma^{+i}\gamma_5 + \tilde{H}_T(x, \xi, t)\frac{\epsilon^{+i\alpha\beta}\Delta_\alpha P_\beta}{M^2} \right. \\ &\quad \left. + E_T(x, \xi, t)\frac{\epsilon^{+i\alpha\beta}\Delta_\alpha\gamma_\beta}{2M} + \tilde{E}_T(x, \xi, t)\frac{\epsilon^{+i\alpha\beta}P_\alpha\gamma_\beta}{M} \right] U(-\vec{q}/2). \end{aligned}$$

Therefore, we have a total of eight leading-twist GPDs for every quark flavor. As with the TMD distributions, the total number is related to the number of independent quark and nucleon scattering amplitudes.

The quantum phase-space distribution $f_\Gamma(\vec{r}, x)$ can be used to construct three-dimensional images of quarks for selected Feynman momenta x in the rest frame of the proton. These images provide the pictures of the proton seen through the Feynman momentum (or "color") filters. To see an example, let us examine the

physical content of $f_{\gamma^+}(\vec{r}, x)$. Working out the spin structure in Equation 27, we find

$$F_{\gamma^+}(x, \xi, t) = [H(x, \xi, t) - \tau E(x, \xi, t)] + i[\vec{s} \times \vec{q}]^z \frac{1}{2M_N} [H(x, \xi, t) + E(x, \xi, t)], \quad 30.$$

where $\tau = \vec{q}^2/4M_N^2$. The first term is independent of the proton spin and generates the phase-space charge density,

$$\rho_+(\vec{r}, x) = \int \frac{d^3\vec{q}}{(2\pi)^3} e^{-i\vec{q}\cdot\vec{r}} [H(x, \xi, t) - \tau E(x, \xi, t)]. \quad 31.$$

The spin-dependent term generates the third component of the phase-space vector current,

$$j_+^z(\vec{r}, x) = \int \frac{d^3\vec{q}}{(2\pi)^3} e^{-i\vec{q}\cdot\vec{r}} i[\vec{s} \times \vec{q}]^z \frac{1}{2M_N} [H(x, \xi, t) + E(x, \xi, t)]. \quad 32.$$

The E-term generates a convection current due to the orbital motion of massless quarks and vanishes when all quarks are in the s-orbit. The physics of separating f_γ^+ into ρ_+ and j_+^z can be seen from the Dirac matrix γ^+ selected by the high-energy probes, which is a combination of time and space components.

Figure 1 shows a model phase-space charge distribution $\rho_+(\vec{r}, x)$ for up quarks (1), to be explained in Section 5. The vertical axis is z, and the three-dimensional images are rotational-symmetric in the x–y plane, for which only a slice is shown as the horizontal axis. Different images are for different Feynman momenta, which in the rest frame are proportional to a special combination of the off-shell energy and momentum along z, $E + k^z$. For further discussion, see Section 5.

By integrating the phase-space charge distribution $\rho_+(\vec{r}, x)$ over x, or superimposing the images at all x, one recovers the spherically symmetric charge density in

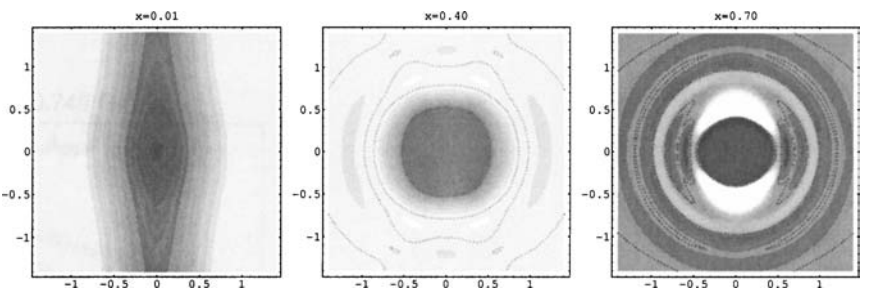

Figure 1 The u-quark phase-space charge distribution at different values of the Feynman momentum from a nonfactorizable parameterization for $H(x, \xi, t)$ (1), with parameters fitted to known form factors and Feynman distributions. The vertical and horizontal axes correspond to z and $|\vec{r}_\perp|$, respectively, measured in fermi.

space. On the other hand, by integrating over x in $j^z_+(\vec{r}, x)$, one obtains the electric current density. In the latter case, if the integral is weighted with x, one obtains the mechanical momentum density (24).

3.5. Impact-Parameter Space

Integrating over the z coordinate in $f_\Gamma(\vec{r}, x)$, one has

$$f_\Gamma(\vec{b}, x) = \int_{-\infty}^{\infty} dz f_\Gamma(\vec{b} = \vec{r}_\perp, z, x) = \int \frac{d^2\vec{q}_\perp}{(2\pi)^2} F_\Gamma(x, 0, -\vec{q}^{\,2}_\perp), \qquad 33.$$

which is related to the GPDs at $\xi = 0$. The distribution f_Γ (introduced in Reference (15); also see Reference (38)) is called impact-parameter-space parton distribution. This distribution has important advantages over a phase-space distribution but also a significant disadvantage.

The important advantages are that $f_\Gamma(\vec{b}, x)$ is a real density in the sense that it is the expectation value of a number operator, and its interpretation does not suffer from relativistic effects. The variables $\vec{b}$ and x live in different dimensions, and therefore there is no quantum mechanical uncertainty constraint. Indeed, $f_\Gamma(\vec{b}, x)$ is a spatial-and-momentum-density hybrid in that it represents a spatial density in the transverse directions and momentum density in the longitudinal direction, and thus is not a Wigner distribution in a proper sense. $f_\Gamma(\vec{b}, x)$ is also invariant under boost along the z direction. In particular, if the nucleon has an infinity momentum, its effective mass is also infinity. Therefore, its spatial structure in the transverse directions, just like in nonrelativistic systems, can be obtained directly from the Fourier transformation of the form factors without the relativistic recoil effects discussed in the previous section.

However, the price one pays for these nice features is one spatial dimension. Every object one studies becomes a pancake in this framework. The physics of ξ in GPDs, which generates the spatial deformation along z from the above discussion, represents a parameter in the process of quantum interference (39–41).

4. PROPERTIES OF GENERALIZED PARTON DISTRIBUTIONS

This section is devoted to a discussion of the general properties of GPDs. Some of these are kinetic, independent of a specific strong-interaction theory—for example, the relations between GPDs and form factors and the usual parton distributions, and the partonic interpretation in light-front quantization. Some properties depend on QCD dynamics, for example, chiral properties, scale evolutions, and large-x and -t behavior. I also emphasize the information about the spin structure of the nucleon contained in GPDs.

4.1. Generalized Form Factors and Polynomiality Condition

One of the most important sources of information about the nucleon structure is the form factors of the electroweak currents. The Pauli form factor F_2 gives the anomalous magnetic moment of the nucleon, $\kappa = F_2(0)$. The charge radius of the nucleon is defined by

$$\langle r^2 \rangle = -6 \left. \frac{dG_E(Q^2)}{dQ^2} \right|_{Q^2=0}, \qquad 34.$$

with $G_E = F_1 - Q^2/(4M^2)F_2$. The axial vector current also defines two form factors,

$$\left\langle P' | \bar{\psi} \gamma^\mu \gamma_5 \psi | P \right\rangle = G_A(Q^2) \bar{U} \gamma^\mu \gamma_5 U + G_P(Q^2) \bar{U} \frac{\gamma_5 q^\mu}{2M} U(P). \qquad 35.$$

The axial form factor $G_A(0)$ at $Q^2 = 0$ is related to the fraction of the nucleon spin carried by the spin of the quarks, $\Delta\Sigma$, and can be measured from polarized DIS and neutrino elastic scattering.

A generalization of the vector and axial-vector currents can be made through the following sets of twist-two operators,

$$\begin{aligned} O_q^{\mu_1 \cdots \mu_n} &= \bar{\psi}_q \gamma^{(\mu_1} i D^{\mu_2} \cdots i D^{\mu_n)} \psi \\ \tilde{O}_q^{\mu_1 \cdots \mu_n} &= \bar{\psi}_q \gamma^{(\mu_1} \gamma_5 i D^{\mu_2} \cdots i D^{\mu_n)} \psi, \end{aligned} \qquad 36.$$

where all indices $\mu_1 \cdots \mu_n$ are symmetric and traceless, as indicated by $(\ldots)$ in the superscripts. These operators form the totally symmetric representation of the Lorentz group. One can similarly introduce the gluon twist-two operators. For $n > 1$, the above operators are not conserved currents from any global symmetry. Consequently, their matrix elements depend on the momentum-transfer scale μ at which they are probed. For the same reason, there is no low-energy probe that couples to these currents.

One can then define the generalized charges $a_n(\mu^2)$ from the forward matrix elements of these currents:

$$\langle P | O^{\mu_1 \cdots \mu_2} | P \rangle = 2a_n(\mu^2) P^{(\mu_1} P^{\mu_2} \cdots P^{\mu_n)}. \qquad 37.$$

The moments of the Feynman parton distribution $q(x, \mu^2)$ are related to these charges as

$$\int_{-1}^{1} dx x^{n-1} q(x, \mu^2) = \int_{0}^{1} dx x^{n-1} [q(x, \mu^2) + (-1)^n \bar{q}(x, \mu^2)] = a_n(\mu^2), \qquad 38.$$

where $\tilde{q}(x, \mu^2)$ is defined in the range $-1 < x < 1$. For $x > 0$, $q(x, \mu^2)$ is simply the density of quarks that carry the fraction x of the parent nucleon momentum. The density of antiquarks is customarily denoted by $\bar{q}(x, \mu^2)$, which in the above notation is $-q(-x, \mu^2)$ for $x < 0$.

One can also define the form factors [$A_{qn,m}(t)$, $B_{qn,m}(t)$, and $C_{qn}(t)$] of these currents using constraints from charge conjugation, parity, time-reversal, and Lorentz symmetries (3):

$$\begin{aligned}
&\langle P'|O_q^{\mu_1\cdots\mu_n}|P\rangle \\
&= \bar{U}(P')\gamma^{(\mu_1}U(P)\sum_{i=0}^{[\frac{n-1}{2}]}A_{qn,2i}(t)\Delta^{\mu_2}\cdots\Delta^{\mu_{2i+1}}\bar{P}^{\mu_{2i+2}}\cdots\bar{P}^{\mu_n)} \\
&\quad+\bar{U}(P')\frac{\sigma^{(\mu_1\alpha}i\Delta_\alpha}{2M}U(P)\sum_{i=0}^{[\frac{n-1}{2}]}B_{qn,2i}(t)\Delta^{\mu_2}\cdots\Delta^{\mu_{2i+1}}\bar{P}^{\mu_{2i+2}}\cdots\bar{P}^{\mu_n)} \\
&\quad+C_{qn}(t)\mathrm{Mod}(n+1,2)\frac{1}{M}\bar{U}(P')U(P)\Delta^{(\mu_1}\cdots\Delta^{\mu_n)}, \qquad 39.
\end{aligned}$$

where $\bar{U}(P')$ and $U(P)$ are Dirac spinors, $\Delta^2=(P'-P)^2=t$, $\bar{P}=(P'+P)/2$, and $\mathrm{Mod}(n+1,2)$ is 1 when n is even and 0 when n is odd. Thus, C_{qn} is present only when n is even. We suppress the renormalization scale dependence for simplicity. Choose a light-light vector n^μ ($n^2=0$) such that

$$n\cdot\bar{P}=1,\quad \xi=-n\cdot\Delta/2. \qquad 40.$$

Then,

$$n_{\mu_1}\cdot n_{\mu_n}\langle P'|O^{\mu_1\cdots\mu_n}|P\rangle = H_n(\xi,t)\bar{U}\not{n}U+E_n(\xi,t)\bar{U}\frac{i\sigma^{\mu\alpha}n_\mu\Delta_\alpha}{2M}U, \qquad 41.$$

where $H_n(\xi,t)$ and $E_n(\xi,t)$ are polynomials in ξ^2 of degree $n/2$ (n even) or $n-1/2$ (n odd). The coefficients of the polynomials are form factors. It is easy to see that they are just the moments of the GPDs $E(x,\xi,t)$ and $H(x,\xi,t)$:

$$\begin{aligned}
\int_{-1}^{1}dx x^{n-1}E(x,\xi,t) &= E_n(\xi,t) \\
\int_{-1}^{1}dx x^{n-1}H(x,\xi,t) &= H_n(\xi,t). \qquad 42.
\end{aligned}$$

Therefore, although GPDs are the functions of two variables, x and ξ, their x^n moment is only a polynomial function of ξ. This is called the polynomiality condition.

More specifically, the first moments of GPDs are constrained by the form factors of the electromagnetic and axial currents. Indeed, by integrating over x, we have (14)

$$\int_{-1}^{1} dx H_q(x,\xi,t) = F_1^q(t), \quad \int_{-1}^{1} dx E_q(x,\xi,t) = F_2^q(t),$$

$$\int_{-1}^{1} dx \tilde{H}_q(x,\xi,t) = G_A^q(t), \quad \int_{-1}^{1} dx \tilde{E}_q(x,\xi,t) = G_P^q(t), \qquad 43.$$

where F_1, F_2, G_A, and G_P are the Dirac, Pauli, axial, and pseudoscalar elastic form factors, respectively. The t-dependence of the form factors is characterized by hadron mass scales, which in turn control the t-dependence of the generalized parton distributions.

4.2. Form Factors of Energy-Momentum Tensor and Spin Structure of the Nucleon

The physical significance of GPDs was first revealed in studying the spin structure of the nucleon (14). Let us review this connection. In the constituent quark model, the nucleon is made of three spin-1/2 quarks moving in the s-orbit. The spin of the nucleon is then a vector sum of the quark spins. Although the simple quark model has been very successful in explaining a large body of experimental data, its prediction about the spin structure has been challenged by the polarized DIS data obtained by the European Muon Collaboration (EMC) (42).

In polarized DIS, a polarized electron exchanges a polarized photon with a polarized nucleon. The polarized photon is absorbed by a polarized quark whose helicity must have the same sign as that of the photon in the center-of-mass frame, or else angular momentum conservation forbids the absorption. Therefore, polarized DIS allows measurement of the polarized quark distributions in the polarized nucleon. From the data taken in a number of recent experiments, along with the analysis of neutron and hyperon β-decay, the fraction of the nucleon spin carried by the quark spin is determined to be (43)

$$\Delta\Sigma(1\,\mathrm{GeV}) = 0.2 \pm 0.1. \qquad 44.$$

This is significantly below the quark model prediction $\Delta\Sigma = 1$.

The fundamental reason for the discrepancy is that the quark model quarks are not the same as the QCD quarks. In DIS, the photons interact directly with the QCD current. Applying the predictions of the constituent quark model to the QCD quarks is at best opportunistic. A more interesting approach to understanding the EMC data is to study the spin structure of the nucleon directly in the fundamental theory. Reference (14) clarified the structure of the angular momentum operator in QCD, from which one can write down a decomposition of the nucleon spin:

$$1/2 = J_q(\mu) + J_g(\mu), \qquad 45.$$

where $J_{q,g}$ are the contributions from the quarks and gluons, respectively. Both contributions are gauge-invariant but renormalization-scale-dependent.

$J_{q,g}(\mu)$ can be expressed as the matrix elements of the QCD energy-momentum tensor $T^{\mu\nu}_{q,g}$:

$$J_{q,g}(\mu) = \left\langle P\frac{1}{2}\left|\int d^3\vec{x}(\vec{x}\times\vec{T}_{q,g})_z\right|P\frac{1}{2}\right\rangle, \qquad 46.$$

which can be extracted from the form factors of the quark and gluon parts of the $T^{\mu\nu}_{q,g}$. Specializing Equation 39 to $n = 2$, one finds

$$\begin{aligned}\left\langle P'\left|T^{\mu\nu}_{q,g}\right|P\right\rangle = \bar{U}(P')\big[&A_{q,g}(t)\gamma^{(\mu}\bar{P}^{\nu)} + B_{q,g}(t)\bar{P}^{(\mu}i\sigma^{\nu)\alpha}\Delta_\alpha/2M \\ &+ C_{q,g}(t)\Delta^{(\mu}\Delta^{\nu)}/M\big]U(P). \qquad 47.\end{aligned}$$

Taking the forward limit of the $\mu = 0$ component and integrating over three-space, one finds that the $A_{q,g}(0)$ give the momentum fractions of the nucleon carried by quarks and gluons, respectively $[A_q(0) + A_g(0) = 1]$. On the other hand, substituting the above into the nucleon matrix element of Equation 46, one finds (14)

$$J_{q,g} = \frac{1}{2}[A_{q,g}(0) + B_{q,g}(0)]. \qquad 48.$$

Therefore, the matrix elements of the energy-momentum tensor provide the fractions of the nucleon spin carried by quarks and gluons. There is an analogy for this. If one knows the Dirac and Pauli form factors of the electromagnetic current, $F_1(Q^2)$ and $F_2(Q^2)$, then the magnetic moment of the nucleon, defined as the matrix element of $(1/2)\int d^3x(\vec{x}\times\vec{j})^z$, is $F_1(0) + F_2(0)$.

Because the quark and gluon energy-momentum tensors are examples of twist-two, spin-two, helicity-independent operators, we immediately have the following sum rule for GPDs (14):

$$\int_{-1}^{1} dx\, x[H_q(x,\xi,t) + E_q(x,\xi,t)] = A_q(t) + B_q(t), \qquad 49.$$

where the ξ dependence, or $C_q(t)$ contamination, drops out. If we extrapolate the sum rule to $t = 0$, the total quark contribution to the nucleon spin is obtained.

The total quark contribution J_q can be decomposed gauge-invariantly into the quark spin $\Delta\Sigma/2$ and orbital contribution L_q:

$$J_q = \Delta\Sigma/2 + L_q. \qquad 50.$$

Knowing J_q and $\Delta\Sigma$, one can extract the quark orbital angular momentum. Thus, a deep understanding of the spin structure of the nucleon can be achieved through the study of GPDs.

4.3. Chiral Properties of GPDs

Because the up and down quark masses are light, QCD has an approximate chiral symmetry in which the left- and right-handed quark fields can rotate independently in flavor space. Strong-interaction phenomenology, however, indicates that the symmetry is spontaneously broken in the vacuum. As a result, the low-energy QCD dynamics is dominated by that of the Goldstone bosons—the pions in this case. One of the obvious manifestations of chiral physics in GPDs is the dominance of the GPD $\tilde{E}$ by the pion pole. Others include the predictions for the pion GPDs and relations between the nucleon and its transition GPDs involving pion emission. This subsection focuses on the fact that chiral perturbation theory allows one to study the chiral behavior of nonperturbative observables such as form factors or parton distributions (44).

The chiral behavior of electromagnetic form factors has been thoroughly investigated in the literature. In some cases, the effects of the Δ-resonances have also been investigated. Similar studies on the form factors of the QCD energy-momentum tensor have been done (45, 46) in the theory with two light flavors. I briefly summarize the results here.

A general strategy in effective theory calculations is operator matching and power counting. This entails matching the quark and gluon operators in QCD to the effective operators in the chiral theory with the same quantum numbers, and then calculating their matrix elements using the chiral Lagrangian. In the singlet case (the sum of the up and down quark contributions), the second-order tensor operator has the following expansion:

$$\mathcal{O}^{\mu_1\mu_2} = f_\pi^2 a_2^\pi \mathrm{Tr}\partial_{\mu_1}\Sigma^\dagger\partial_{\mu_2}\Sigma + a_2^N(2M)v_{\mu_1}v_{\mu_2}\bar{N}_v N_v + b_2^N(2)(i\partial_\alpha)v_{\mu_1}\bar{N}_v[S_{\mu_2}, S_\alpha]N_v + c_2^N\frac{1}{2M}(i\partial^{\mu_1})(i\partial^{\mu_2})\bar{N}_v N_v + \ldots, \quad 51.$$

where ellipses denote higher dimensional operators. $\Sigma = \exp(i\pi^a\tau^a/f_\pi)$ and N_v are the nonlinear representations of the pion and nucleon fields, respectively; v_μ and M are the velocity and mass of the nucleon ($f_\pi = 93$ MeV). The coefficients of the operators summarize the short-distance physics and are a priori unknown.

From the above, one can calculate the leading nonanalytical chiral contribution to the gravitational form factors (46),

$$A(Q^2) - \frac{Q^2}{4M^2}B(Q^2) = a_2^N + 3a_2^\pi\frac{g_A^2}{64\pi f_\pi^2 M} \times \left[\left(2m_\pi^2 - Q^2\right)\int_0^1 dx\sqrt{m_\pi^2(x)} + \frac{4}{3}m_\pi^2\right]$$

$$A(Q^2)+B(Q^2)=b_2^N+3\frac{g_A^2}{(4\pi f_\pi)^2}\int_0^1\left(a_2^\pi m_\pi^2(x)-b_2^N m_\pi^2\delta(x)\right)\ln\frac{m_\pi^2(x)}{\Lambda^2}$$

$$C_2(Q^2)=c_2^N+3a_2^\pi\frac{g_A^2}{16\pi f_\pi^2}M\left(2m_\pi^2-Q^2\right)\int_0^1 dx\frac{x(1-x)}{\sqrt{m_\pi^2(x)}},\quad 52.$$

where $m_\pi(x)=m^2-x(1-x)Q^2$ and Λ^2 is the chiral cutoff, on the order of $4\pi f_\pi$. The first combination contains chiral-singular terms such as m_π^3 or $m_\pi Q^2$, the second $m_\pi^2\ln m_\pi^2$ and $Q^2\ln m_\pi$, and the third m_π and Q^2/m_π. This indicates that the nucleon mass radius has a contribution scaling as m_π, whereas the momentum density radius diverges like $\ln m_\pi$. One application of the above results is to the chiral behavior of the quark or gluon contribution to the nucleon spin (45),

$$J_q(m_\pi)=b_2^N+3\left(a_2^\pi-b_2^N\right)\frac{g_A^2m_\pi^2}{(4\pi f_\pi)^2}\ln\frac{m_\pi^2}{\Lambda^2},\quad 53.$$

which can be used, for example, to extrapolate the lattice results at nonphysical quark masses to physical ones.

4.4. Partonic Interpretation

From their definition, it is straightforward to see that in the limit $\xi\to 0$ and $t\to 0$, GPDs reduce to ordinary parton distributions. For instance,

$$H_q(x,0,0)=q(x),$$
$$\tilde{H}_q(x,0,0)=\Delta q(x),\quad 54.$$

where $q(x)$ and $\Delta q(x)$ are the unpolarized and polarized quark densities. Similar equations hold for gluon distributions. For practical purposes, in the kinematic region where

$$\sqrt{|t|}\ll M_N\quad\text{and}\quad\xi\ll x,\quad 55.$$

an off-forward distribution may be approximated by the corresponding forward one. The first condition, $\sqrt{|t|}\ll M_N$, is crucial—otherwise there is a significant form-factor suppression that cannot be neglected at any x and ξ. For a given t, ξ is restricted to

$$|\xi|<\sqrt{-t/(M^2-t/4)}.\quad 56.$$

Therefore, when $\sqrt{|t|}$ is small, ξ is automatically limited, and there is in fact a large region of x where the forward approximation holds.

The parton content of GPDs is made transparent in light-cone coordinates and light-cone gauge. To see this, let us recall

$$F_{\gamma^+} = \frac{1}{2}\int \frac{d\lambda}{2\pi} e^{i\lambda x} \left\langle P' \left| \overline{\psi}_q \left(-\frac{\lambda}{2}n\right) \not{n} \mathcal{P} e^{-ig\int_{\lambda/2}^{-\lambda/2} d\alpha\, n\cdot A(\alpha n)} \psi_q\left(\frac{\lambda}{2}n\right) \right| P \right\rangle, \quad 57.$$

where the gauge-link operator is explicitly shown. In the light-cone gauge $n \cdot A = 0$, the gauge link between the quark fields can be ignored. Using the light-cone coordinate system

$$x^{\pm} = \frac{1}{\sqrt{2}}(x^0 \pm x^3); \quad x_\perp = (x^1, x^2), \quad 58.$$

we can expand the Dirac field as follows:

$$\psi_+(x^-, x_\perp) = \int \frac{dk^+ d^2\vec{k}_\perp}{2k^+(2\pi)^3}\theta(k^+) \sum_{\lambda=\pm} \Big(b_\lambda(k^+, \vec{k}_\perp)u_\lambda(k)e^{-i(x^-k^+ - \vec{x}_\perp\cdot\vec{k}_\perp)}$$
$$+ d_\lambda^\dagger(k^+, \vec{k}_\perp)v_\lambda(k)e^{i(x^-k^+ - \vec{x}_\perp\cdot\vec{k}_\perp)}\Big), \quad 59.$$

where $\psi_+ = P_+\psi$ and $P_\pm = \frac{1}{2}\gamma^\mp\gamma^\pm$. The quark (antiquark) creation and annihilation operators, $b_{\lambda k}^\dagger$ ($d_{\lambda k}^\dagger$) and $b_{\lambda k}$ ($d_{\lambda k}$), obey the usual commutation relation. Substituting the above into Equation 57, we have (62)

$$F_q(x,\xi) = \frac{1}{2p^+V}\int \frac{d^2k_\perp}{2\sqrt{|x^2-\xi^2|}(2\pi)^3} \sum_\lambda$$
$$\times \begin{cases} \langle P'|b_\lambda^\dagger((x-\xi)p^+, \vec{k}_\perp + \vec{\Delta}_\perp)b_\lambda((x+\xi)p^+, \vec{k}_\perp)|P\rangle, \\ \qquad\qquad\qquad\qquad \text{for } x > \xi \\ \langle P'|d_\lambda((-x+\xi)p^+, -\vec{k}_\perp - \vec{\Delta}_\perp)b_{-\lambda}((x+\xi)p^+, \vec{k}_\perp)|P\rangle, \\ \qquad\qquad\qquad\qquad \text{for } \xi > x > -\xi \\ -\langle P'|d_\lambda^\dagger((-x-\xi)p^+, \vec{k}_\perp + \vec{\Delta}_\perp)d_\lambda((-x+\xi)p^+, \vec{k}_\perp)|P\rangle, \\ \qquad\qquad\qquad\qquad \text{for } x < -\xi \end{cases} \quad 60.$$

where V is a volume factor. The distribution has different physical interpretations in the three different regions. In the region $x > \xi$, it is the amplitude for taking a quark of momentum k out of the nucleon, changing its momentum to $k + \Delta$, and inserting it back to form a recoiled nucleon. In the region $\xi > x > -\xi$, it is the amplitude for taking out a quark and antiquark pair with momentum $-\Delta$. Finally, in the region $x < -\xi$, we have the same situation as in $x > \xi$, except the quark is replaced by an antiquark. The first and third regions are similar to those present in ordinary parton distributions [called the Dokshitzer-Gribov-Lipatov-Altarelli-Parisi (DGLAP) region], whereas the middle region is similar to that in a meson amplitude [the Efremov-Radyushkin-Brodsky-Lepage (ERBL) region].

A partonic interpretation can also be made by transforming the nucleon states to those in the impact-parameter space (40).

4.5. Scale Evolution

Like ordinary parton distributions, GPDs depend on the renormalization scale, which, in practical applications, can be taken to be the probing scale. The scale evolution of GPDs contains rich physics and interpolates between the evolutions of a parton distribution and a meson distribution amplitude (13). There is a huge literature on this subject and the evolution kernal is now completely known up to two loops.

For simplicity, I present here an example of the scale evolution of the nonsinglet distribution F_{γ^+}. According to Equation 60, it is natural that the distributions in three different kinematic regions evolve differently. In the region $x > \xi$, where we have a quark creation and annihilation, the evolution equation is

$$\frac{D_Q F_{NS}(x,\xi,Q^2)}{D\ln Q^2} = \frac{\alpha_s(Q^2)}{2\pi}\int_x^1 \frac{dy}{y} P_{NS}\left(\frac{x}{y},\frac{\xi}{y},\frac{\epsilon}{y}\right) F_{NS}(y,\xi,Q^2), \qquad 61.$$

where

$$\frac{D_Q}{D\ln Q^2} = \frac{d}{d\ln Q^2} - \frac{\alpha_s(Q^2)}{2\pi} C_F \left[\frac{3}{2} + \int_\xi^x \frac{dy}{y-x-i\epsilon} + \int_{-\xi}^x \frac{dy}{y-x-i\epsilon}\right]. \qquad 62.$$

The parton splitting function is

$$P_{NS}(x,\xi,\epsilon) = C_F \frac{x^2+1-2\xi^2}{(1-x+i\epsilon)(1-\xi^2)}. \qquad 63.$$

The end-point singularity is cancelled by the divergent integrals in $D_Q/D\ln Q^2$. Obviously, when $\xi = 0$, the splitting function becomes the DGLAP evolution kernel (47). For $-\xi < x < \xi$, where we have creation or annihilation of a quark-antiquark pair, the evolution takes the form

$$\frac{D_Q F_{NS}(x,\xi,Q^2)}{D\ln Q^2} = \frac{\alpha_s(Q^2)}{2\pi}\left[\int_x^1 \frac{dy}{y} P'_{NS}\left(\frac{x}{y},\frac{\xi}{y},\frac{\epsilon}{y}\right) - \int_{-1}^x \frac{dy}{y} P'_{NS}\left(\frac{x}{y},-\frac{\xi}{y},\frac{\epsilon}{y}\right)\right] F_{NS}(y,\xi,Q^2), \qquad 64.$$

where

$$P'_{NS}(x,\xi,\epsilon) = 2C_F \frac{x+\xi}{\xi(1+\xi)}\left(1+\frac{2\xi}{1-x+i\epsilon}\right). \qquad 65.$$

When $\xi = 1$, the kernel reduces to the Brodsky & Lepage kernel (49). For $x < -\xi$, where we have antiquark creation and annihilation, the evolution takes the same form as Equation 61, apart from the replacement $\int_x^1 \to -\int_{-1}^x$.

One can also understand the above evolution from the viewpoint of local operators. In the operator form, the evolution has been studied at the leading logarithmic approximation. For a given twist-two operator of spin n shown in Equation 36, it in general mixes with the following operators of total derivatives:

$$\mathcal{O}^{\mu_1\cdots\mu_n}_{n,2i} = i\partial^{(\mu_1}\cdots i\partial^{\mu_{2i}}\bar{\psi} i\overset{\leftrightarrow}{\mathcal{D}}^{\mu_{2i+1}}\cdots i\overset{\leftrightarrow}{\mathcal{D}}^{\mu_{n-1}}\gamma^{\mu_n)}\psi. \quad 66.$$

Consideration of such mixing is already necessary in studying the evolution of the leading-twist meson wave functions. The answer was first obtained by Efremov & Radyushkin (48) and by Brodsky & Lepage (49). Actually, at the leading logarithmic order, the answer may be guessed from the naive conformal symmetry of perturbative QCD (pQCD), which is broken by quantum effects only at the next-to-leading logarithmic order. The following combination of the twist-two operators furnishes a representation of the special conformal symmetry group,

$$\tilde{\mathcal{O}}_n = (i\partial\cdot n)^{n-1}\bar{\psi}C^{3/2}_{n-1}\left(\frac{i\overset{\leftrightarrow}{\mathcal{D}}\cdot n}{i\overset{\leftarrow}{\partial}\cdot n + i\overset{\rightarrow}{\partial}\cdot n}\right)\not{n}\psi, \quad 67.$$

where the $C^{3/2}_{n-1}(x)$ are the Gegenbauer polynomials of order 3/2. Its evolution takes exactly the diagonal form of that for the operator without the total derivatives (48):

$$\tilde{\mathcal{O}}_n(\mu_1) = \left(\frac{\alpha_s(\mu_1)}{\alpha_s(\mu_2)}\right)^{\frac{\gamma_n}{2\beta_0}}\tilde{\mathcal{O}}_n(\mu_2), \quad 68.$$

where

$$\gamma_n = 2C_F\left[4\sum_{i=1}^{n}\frac{1}{i} - 3 - \frac{2}{n(n+1)}\right], \quad 69.$$

and $\beta_0 = 11 - 2n_f/3$. $C_F = 4/3$ for the SU(3) color group, and n_f is the number of light quark flavors. For the leading-twist pion wave function, the above result leads to a general expansion in terms of Gegenbauer polynomials.

In a series of interesting publications, Belitsky & Müller have presented the evolution of GPDs at two loops (50). The key observation is again that pQCD is approximately conformally invariant. The breaking of the conformal symmetry can be studied through the conformal Ward identities, which allow one to obtain the nontrivial part of the two-loop anomalous dimensions by calculating only the one-loop conformal anomaly.

4.6. Inequalities

From their parton content, GPDs may be regarded as the interferences of quantum mechanical amplitudes of finding partons in a hadron. According to the positivity condition on the norm of any physical state, one can derive inequalities for GPDs, as first observed by Martin & Ryskin (51). The most extensive investigation on the GPD inequalities has been carried out in a series of papers by Poblytsa

(52). Subtleties involving scale evolution and direct derivation from physical cross sections have also been discussed. The inequalities can be used as constraints in parameterizing GPDs phenomenologically.

All inequalities involving twist-two GPDs and the usual Feynman parton distributions in the nucleon can be derived from the condition (52)

$$\left\| \sum_{k=1}^{2} \sum_{\lambda\mu} c_{\lambda\mu}^{(k)} \int \frac{d\tau}{2\pi} e^{i\tau x_k (P_k n)} \phi_\mu (\tau n) \, |P_k, \lambda\rangle \right\|^2 \geq 0. \qquad 70.$$

Here $|P_k, \lambda\rangle$ is the nucleon state with momentum P_k and polarization λ, while ϕ_μ is the component of the quark (or gluon) field that corresponds to the polarization μ. Introducing the quark-nucleon helicity amplitudes,

$$A_{\lambda'\mu',\lambda\mu} = \int \frac{dz^-}{2\pi} e^{ixP^+z^-} \langle p', \lambda' | O_{\mu',\mu}(z) | p, \lambda \rangle \Big|_{z^+=0, z^\perp=0}, \qquad 71.$$

where $O_{\mu',\mu}$ are bilinear quark light-ray operators with the polarization indices μ, μ'. A's contain all the leading-twist GPDs. Now the positivity condition is easily translated into the condition for the following 8×8 matrix:

$$\begin{pmatrix} A(x_1, 0, 0) & A^\dagger(x, \xi, t) \\ A(x, \xi, t) & A(x_2, 0, 0) \end{pmatrix} \geq 0 \,. \qquad 72.$$

where A's are 4×4 matrices in quark and proton helicity space.

The above equation can be used to derive a host of inequalities for individual GPDs or any linear combination of them. For example, an inequality that involves $\tilde{H}$ and $\tilde{E}$ reads,

$$\left| H^q - \frac{\xi^2}{1-\xi^2} E^q \right| \leq \frac{1}{4\sqrt{1-\xi^2}} \times \left\{ \sqrt{(q + \Delta q - 2\delta q)_{x_1} (q + \Delta q - 2\delta q)_{x_2}} \right.$$

$$\left. + \sqrt{(q + \Delta q + 2\delta q)_{x_1} (q + \Delta q + 2\delta q)_{x_2}} + 2\sqrt{(q - \Delta q)_{x_1} (q - \Delta q)_{x_2}} \right\}, \qquad 73.$$

where subscripts $x_1 = x + \xi/(1+\xi)$ and $x_2 = x - \xi/(1-\xi)$ are shorthand for arguments, and $q(x)$, $\Delta q(x)$, and $\delta q(x)$ are quark unpolarized, helicity, and transversity distributions, respectively. However, when averaging over the quark polarization, one finds

$$\left| H^q(x, \xi, t) - \frac{\xi^2}{1-\xi^2} E^q(x, \xi, t) \right| \leq \sqrt{\frac{q(x_1) q(x_2)}{1-\xi^2}}, \qquad 74.$$

which was first obtained in Reference (53). Two examples of inequalities involving the individual GPD and unpolarized quark distributions are

$$|E^q(x, \xi, t)| \leq \frac{2m}{\sqrt{t_0 - t}} \sqrt{q(x_1) q(x_2)}, \qquad 75.$$

$$|H^q(x,\xi,t)| \leq \sqrt{\left(1+\frac{-t_0\xi^2}{t_0-t}\right)\frac{q(x_1)q(x_2)}{1-\xi^2}}, \qquad 76.$$

where $t_0 = -4\xi^2 m^2/(1-\xi^2)$.

More general inequalities can be derived that involve GPDs convoluted with arbitrary functions. Poblytsa has shown how to parameterize GPDs to satisfy both the general positivity constraints and the polynomiality conditions (52).

4.7. GPDs at Large x and t

Like Feynman parton distributions at large x and electromagnetic form factors at large t, the GPDs at large x and t can be studied in pQCD. In the $x \to 1$ limit, Yuan finds (54)

$$H_q(x,\xi,t) \to (1-x)^3/(1-\xi^2)^2$$
$$E_q(x,\xi,t) \to (1-x)^5/(1-\xi^2)^4 f(\xi), \qquad 77.$$

where $f(\xi)$ is an unknown function. Thus, the distributions are independent of the momentum transfer t in the limit. According to Equation 25, this implies that the transverse profile of the quarks shrinks to zero. This makes sense intuitively because when a quark carries all the longitudinal momentum of a nucleon, its center of gravity must coincide with that of the nucleon (15). Perturbative arguments also show that any t-dependence is suppressed by $(1-x)^2$, or goes like $t(1-x)^2$ [(54); see also (55)].

In the large-t limit, one can derive a pQCD factorization formula for GPDs. Let us consider first the pion case (56, 57). The leading pQCD contribution is shown in Figure 2, where the initial and final pion states are replaced by the light-cone Fock component with the minimal number of partons. The circled crosses in the diagrams represent the bilocal quark operator. The hard part responsible for the large momentum transfer contains a single gluon exchange just like in the electromagnetic form factor. In the first two diagrams (a) and (b), there is a hard gluon exchange between the two quark lines, and in the third one, there is a gluon coming from the gauge link. Because the transverse momenta of the quarks are expected to be on the order of $\Lambda_{\rm QCD}$, we may ignore them in calculating the hard part. Thus, we can effectively integrate out $k_\perp$ in the pion wave function to obtain the distribution amplitude, $\phi(x) = \int \frac{d^2k_\perp}{(2\pi)^3}\psi(x,k_\perp)$. The parton transverse momenta flowing into the hard part are now taken to be zero.

The result of the above pQCD analysis is a factorization formula for the GPD at large t in terms of the quark distribution amplitude (57),

$$H_q(x,\xi,t,\mu) = \int dx_1 dy_1 \phi^*(y_1,\mu)\phi(x_1,\mu)T_{Hq}(x_1,y_1,x,\xi,t,\mu), \qquad 78.$$

where T_{Hq} is the hard part and can be calculated as a perturbation series in α_s. All quantities in the above equation depend on the renormalization scale μ. The

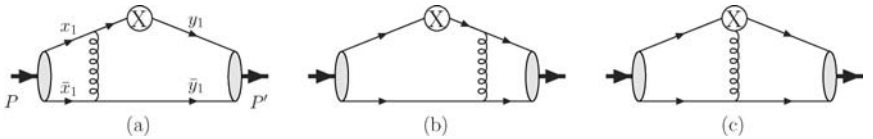

Figure 2 Leading pQCD diagrams contributing to the pion's generalized parton distribution $H(x, \xi, t)$ at large $-t$. The circled crosses represent the nonlocal quark operator.

μ-dependence in the hard part must be sufficient to account for the difference between the GPD and the distribution amplitude.

The leading contribution to the hard part can be calculated straightforwardly:

$$T_u(x, x_1, y_1) = \frac{4\pi\alpha_s C_F}{\bar{x}_1\bar{y}_1(-t)}\delta(x-\lambda_1)\left[(1-\xi)+\frac{1-\xi^2}{\lambda_1-\tilde{\lambda}_1}\right]+\text{h.c.}, \qquad 79.$$

where $C_F = 4/3$, h.c. stands for a term obtained by exchanging x_i and y_i, and ξ and $-\xi$, $\lambda_1 = y_1 + \bar{y}_1\xi$, $\tilde{\lambda}_1 = x_1 - \bar{x}_1\xi$, where $\bar{x} = 1 - x$. Because $0 < y_1 < 1$, the first term contributes when $x > \xi$; the second term contributes when $x > -\xi$, which indicates an up–anti-up pair contribution. The antiquark is generated through the one-gluon exchange on the top of the valence wave function. The GPD for the down quark $H_d(x, \xi, t)$ can be obtained from that of the up quark through simple charge symmetry, $H_d(x, \xi, t) = -H_u(-x, \xi, t)$.

The above result can be translated into one for the moments of the GPDs $H_q^{(n)}(\xi, t) = \int_{-1}^{1} dx x^{n-1} H_q(x, \xi, t)$. In fact, the factorization formula applies for the individual moments, $H_q^{(n)}(\xi, t) = \int dx_1 dy_1 \phi^*(y_1)\phi(x_1) T_{Hq}^{(n)}(x_1, y_1, \xi, t)$, where $T_{Hq}^{(n)}(x_1, y_1, \xi, t)$ is simply the nth moment of $T_{Hq}(x_1, y_1, x, \xi, t)$. For the up quark in the pion, we have

$$T_u^{(n)}(\xi, t) = \frac{4\pi\alpha_s C_F}{\bar{x}_1\bar{y}_1(-t)}\left[(1-\xi)\lambda_1^{n-1}+(1+\xi)\tilde{\lambda}_1^{n-1}+(1-\xi^2)\sum_{m=0}^{n-2}\lambda_1^m\tilde{\lambda}_1^{n-m-2}\right], \qquad 80.$$

which contains both even and odd powers of ξ. For $n = 1$, the above reproduces the hard part in the QCD factorization formula for the pion form factor. For $n = 2$, $T_u^{(2)}(\xi, t) = 4\pi\alpha_s C_F/(\bar{x}_1\bar{y}_1 t)\left[(x_1 + y_1 + 1) + 2(x_1 - y_1)\xi + (x_1 + y_1 - 3)\xi^2\right]$. It is easy to see that the linear dependence in ξ does not contribute to $H_u^{(1)}(\xi, t)$ because of the symmetry in the initial and final states. For the same reason, all odd powers of ξ in $T_u^{(n)}$ do not contribute to the GPD moments.

For the nucleon, the factorization formula for the GPD H_q takes a similar form:

$$H_q(x, \xi, t) = \int [dx][dy]\Phi_3^*(y_1, y_2, y_3)\Phi_3(x_1, x_2, x_3) T_{Hq}(x_i, y_i, x, \xi, t), \qquad 81.$$

where $[dx] = dx_1 dx_2 dx_3 \delta(1 - x_1 - x_2 - x_3)$, and $\Phi_3(x_i)$ is the three-quark distribution amplitude (see, e.g., Reference 58. The leading-order hard kernel can be found in Reference 57).

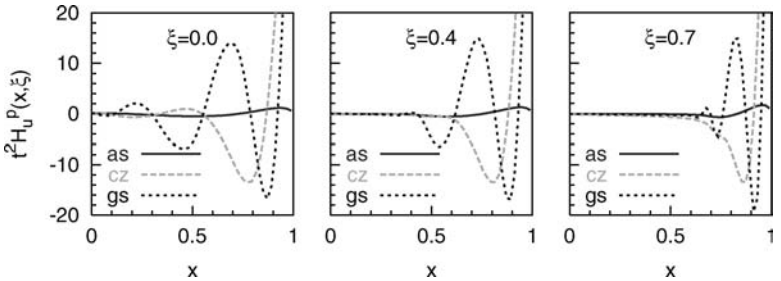

Figure 3 $t^2 H_u(x, \xi, t)$ for the proton at $-t = 20$ GeV^2. CZ refers to the Chernyak-Zhitnitsky amplitude, GS the Gari-Stefanis amplitude, and AS the asymptotic amplitude.

One can make a numerical calculation of $H_u(x, \xi, t)$ using various model amplitudes in the literature (59, 60). Using the strategy of Reference (61), one can compute $t^2 H_u$, as shown in Figure 3, for three different values of ξ at $t^2 = -20\,\text{GeV}^2$ with the asymptotic, Chernyak-Zhitnitsky (CZ), and Gari-Stefanis (GS) amplitudes. Although the CZ and GS amplitudes both give reasonable accounts of data on F_1^p for $-t \geq 10$ GeV^2, the two yield very different predictions for the GPD. Note that the scale of H_u is strikingly large; a relatively small Dirac F_1 results from the cancellation in the integration.

5. GPDs FROM HARD SCATTERING, LATTICE QCD, AND MODELS

GPDs are nonperturbative nucleon observables, and apart from the general properties discussed in the previous section, we know little about the dynamical information encoded in them. This section considers several approaches to gain access to them. First is experimental measurement. It is fortunate that there exists a new class of hard processes in which GPDs can be measured and/or constrained. The simplest is called deeply virtual Compton scattering (DVCS). GPDs can also be calculated in QCD using the lattice field theory method, just like ordinary parton distributions. Since the bilocal operators in GPDs involve real-time correlation, only the moments of GPDs, or generalized form factors, are directly computable. Finally, one may learn certain dynamical features of GPDs in various nucleon models. A more phenomenological approach, GPD modeling, parameterizes the GPDs using various constraints and fits the parameters to experimental and lattice QCD data.

5.1. Hard Exclusive Processes

In recent years, the search for an experimental measurement of GPDs has turned up a new class of QCD hard scattering processes. The simplest, and possibly the most promising, is deep-inelastic exclusive production of photons, mesons, and even lepton pairs. Let us consider briefly two experiments that have been studied extensively in the literature: DVCS, in which a real photon is produced,

and diffractive meson production. Both processes have practical advantages and disadvantages. Real photon production is, in a sense, cleaner but the cross section is reduced by an additional power of $\alpha_{\rm em}$. The Bethe-Heitler contribution can be important but can actually be used to extract the DVCS amplitude through interferences, as in a single-spin asymmetry. Meson production may be easier to detect, but it has a twist suppression of $1/Q^2$. In addition, the theoretical cross section depends on the unknown leading light-cone wave function of the mesons.

DVCS was first proposed (14, 62) as a practical way to measure the generalized distributions. Consider virtual photon scattering in which the momenta of the incoming (outgoing) photon and nucleon are $q(q')$ and $P(P')$, respectively. The Compton amplitude is defined as

$$T^{\mu\nu} = i \int d^4z e^{\bar{q}\cdot z} \left\langle P' \left| \mathrm{T} J^\mu \left(-\frac{z}{2}\right) J^\nu \left(\frac{z}{2}\right) \right| P \right\rangle, \qquad 82.$$

where $\bar{q} = (q + q')/2$. In the Bjorken limit, $-q^2$ and $P \cdot q \to \infty$ and their ratio remains finite; the scattering is dominated by the single-quark process, in which a quark absorbs the virtual photon, immediately radiates a real one, and falls back to form the recoiling nucleon. In the process, the initial and final photon helicities remain the same. The leading-order Compton amplitude is then

$$T^{\mu\nu} = g_\perp^{\mu\nu} \int_{-1}^{1} dx \left(\frac{1}{x - \xi + i\epsilon} + \frac{1}{x + \xi - i\epsilon}\right) \sum_q e_q^2 F_q(x, \xi, t, Q^2) \qquad 83.$$

$$+ i\epsilon^{\mu\nu\alpha\beta} p_\alpha n_\beta \int_{-1}^{1} dx \left(\frac{1}{x - \xi + i\epsilon} - \frac{1}{x + \xi - i\epsilon}\right) \sum_q e_q^2 \tilde{F}_q(x, \xi, t, Q^2),$$

where n and p are the conjugate light-cone vectors defined according to the collinear direction of $\bar{q}$ and $\bar{P}$, and $g_\perp^{\mu\nu}$ is the metric tensor in transverse space. ξ is related to the Bjorken variable $x_B = -q^2/(2P \cdot q)$ by $x_B = 2\xi/(1 + \xi)$.

Much theoretical work has been devoted to DVCS in the past few years. For example, an all-order perturbative proof that DVCS is factorizable has been found. Belitsky, Müller, and Kirchner have worked out, up to twist-two and -three orders, comprehensive expressions for cross sections and spin asymmetries involving polarized beam and target (63, 64). The time-like virtual-photon (or lepton-pair) production has recently been studied (65, 66).

Development on the experimental front is also promising. Recently, both ZEUS and H1 collaborations have announced the first evidence for a DVCS signature, and the HERMES collaboration at DESY and the CLAS collaboration at JLab have made the first measurements of the DVCS single-spin asymmetry (67). More experiments are planned for COMPASS, JLab, and future facilities.

Another process sensitive to GPDs is deep-inelastic exclusive vector-meson production. This was studied by Brodsky et al. (68), but they neglected the off-forward nature of the two gluon exchanges. The scattering amplitude in terms of the

generalized gluon distribution was first found by Radyushkin (69). With the virtual photon and vector meson both polarized longitudinally (i.e., determined through a Rosenbluth separation, with the vector meson polarization measured via its decay products), one finds

$$\frac{d\sigma_{LL}}{dt}(\gamma^* N \to VN) = \frac{4\pi\Gamma_V m_V \alpha_s^2(Q)\eta_V^2}{3\alpha_{\rm em} Q^6} \times \left| 2x_B \int_{-1}^{1} dx \left(\frac{1}{x-\xi+i\epsilon} + \frac{1}{x+\xi-i\epsilon} \right) F_g(x,\xi,t) \right|^2, \qquad 84.$$

where again $x_B = 2\xi/(1+\xi)$. The above formula is valid for any x_B and t smaller than typical hadron mass scales. Later, Collins et al. (70) showed that exclusive meson production in DIS is factorizable to all orders in perturbation theory. The reader can find more detailed results in experiment and theory in Reference (2).

5.2. Lattice QCD

As nucleon matrix elements, GPDs must be calculable in the fundamental theory. At present, our only way to compute, rather than model, QCD dynamics is lattice field theory. Such significant breakthroughs in lattice QCD have been made in the past decade that accurate evaluations of the nucleon matrix elements might be possible in the near future.

Exploratory calculations for electromagnetic form factors have been made since the early 1990s. Calculations of the form factors of higher spin operators are essentially similar. The first lattice calculation of form factor $A_2(Q^2)+B_2(Q^2)$ was performed in the quenched approximation with Wilson fermions (71). The lattice size was $16^3 \times 24$ with coupling $\beta = 6.0$ corresponding to lattice spacing of about $1.7 \sim 2.1$ GeV^{-1}. The lattice up and down quark masses were approximately 370, 210, 120, and 80 MeV/c^2, and the results were linearly extrapolated to the chiral limit. The Q^2 dependence was fitted to a dipole form and the result was used to find the form factor at $Q^2 = 0$, which, as discussed above, is the fraction of the nucleon spin carried by quarks. The result is $J_q = 0.30 \pm 0.07$ at $\overline{\rm MS}$ scale 1.8 GeV, in which the contribution from the disconnected vacuum polarization diagram is also included. $A_2(Q^2) + B_2(Q^2)$ at $Q^2 = 0$ has also been calculated directly (72) without using Q^2 extrapolation. The result $J_q = 0.35 \pm 0.09$ was found at the quark mass $m_q = 210$ MeV with similar lattice configurations.

More recently, the QCDSF collaboration has carried out similar quenched calculations with $\mathcal{O}(a)$-improved Wilson fermions on a slightly larger lattice of $16^3 \times 32$ (73). The energy-momentum form factors $A_2(Q^2)$, $B_2(Q^2)$, and $C_2(Q^2)$ were calculated separately as functions of discrete Q^2. A common dipole mass was used to parameterize the Q^2 dependence and was fitted to be 1.1(2) GeV. Extrapolation to the chiral limit and $Q^2 = 0$ yielded $J_{u+d} = 0.33 \pm 0.07$ without the contribution from the vacuum insertion.

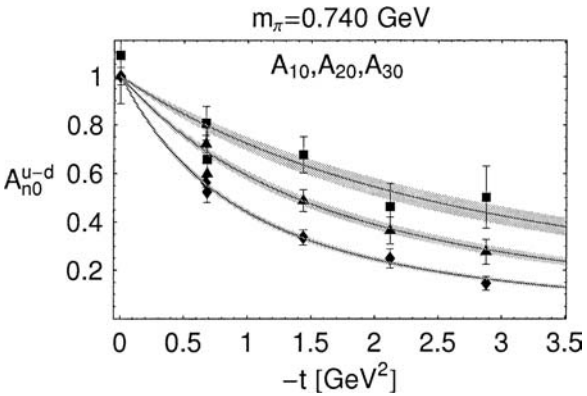

Figure 4 The generalized form factors from a dynamical simulation of QCD on the lattice with a large quark mass (74). The form factors become harder as the spin of the operator increases.

A first dynamical calculation of the generalized form factors was made by the LHPC and SESAM collaborations (74). The quarks in the calculations had quite heavy masses, about 750 and 900 MeV/c^2. Form factors A_{n0} for quark spin-independent twist-two operators and $\tilde{A}_{n0}$ for quark spin-dependent twist-two operators were calculated for $n = 1, 2, 3$. The singlet B_2 form factor is consistent with zero within the statistical errors. It was also found that the form factor becomes harder as the spin of the operators n increases (see Figure 4).

One of the primary goals of lattice simulation is to bring down the quark masses to the physical ones so that the Goldstone boson (pion) physics can be correctly and fully incorporated.

5.3. GPDs from Nucleon Models and Parameterizations

Given a nucleon model with quark degrees of freedom, one can calculate the generalized quark distributions in the model. This has been done, for example, in the MIT bag model (75), the chiral-quark soliton model (76, 77), and more recently in the nonrelativistic quark models (78). These calculations may provide some guidance on the functional dependence of GPDs, particularly if a model is constrained to reproduce electromagnetic form factors and ordinary parton distributions. However, the quarks in these models are not the QCD quarks, even at low renormalization scale, and no rigorous relation between the two has ever been established.

A more phenomenological approach is to parameterize the (light-cone) wave functions and fit the parameters to various nucleon observables. There is no Lagrangian or Hamiltonian involved, and therefore the dynamical origin of these wave functions is unclear. However, this is a very economical way to correlate hadronic observables.

This subsection mainly focuses on a GPD parameterization that takes into account a set of constraints (1). An approach like this one is important to extract information about GPDs from experimental data, just as in the case of Feynman parton distributions. All or some of the known conditions can be imposed on a parameterization—for example, the large and small x and t behavior, positivity constraint, polynomiality condition, sum rules, etc. Finally, one can fit the parameters to experimental data or lattice QCD results.

The simplest way to satisfy the polynomiality condition is to relate it to a double distribution $F(y, x, t)$ (80) and the D-term (77):

$$H(x,\xi,t) = \int_{-1}^{1} \frac{dy}{\xi}\, \Xi(y|x,\xi) F\left(y, \frac{x-y}{\xi}, t\right) + \theta(\xi > |x|) D\left(\frac{x}{\xi}, t\right). \quad 85.$$

The "step"-function kernel in Equation 85 has the form

$$\Xi(y|x,\xi) = \theta(x>\xi)\theta\left(\frac{x+\xi}{1+\xi} \geq y \geq \frac{x-\xi}{1-\xi}\right)$$

$$+\theta(-\xi > x)\theta\left(\frac{x+\xi}{1-\xi} \geq y \geq \frac{x-\xi}{1+\xi}\right) + \theta(\xi > |x|)\theta\left(\frac{x+\xi}{1+\xi} \geq y \geq \frac{x-\xi}{1+\xi}\right).$$

The q-flavor double distribution $F_q = F_q^{\text{val}} + F_q^{\text{sea}}$, including both valence and sea, is assumed to be related to the non-forward quark distribution $f_q(y, t)$ through a profile function $\pi(y, z, b)$:

$$F_q^{\text{val}}(y,z,t) = f_q^{\text{val}}(y,t)\theta(y)\pi(|y|, z; b_{\text{val}}), \quad 86.$$

$$F_q^{\text{sea}}(y,z,t) = (\bar{f}_q(y,t)\theta(y) - \bar{f}_q(-y,t)\theta(-y))\pi(|y|, z; b_{\text{sea}}), \quad 87.$$

where at $t = 0$ the function $f_q(y, t = 0)$ reduces to the conventional parton distribution functions. The profile function with a single parameter b is assumed to be universal for valence- and sea-quark species, and reads (80)

$$\pi(y,z;b) = \frac{\Gamma(b+3/2)}{\sqrt{\pi}\Gamma(b+1)} \frac{[(1-y)^2 - z^2]^b}{(1-y)^{2b+1}}. \quad 88.$$

To proceed further, one designs a nonfactorized ansatz (4, 41, 81) for the functions $f_q(y, t)$ with intertwined t and y dependence. The model is based on the Gluck-Reya-Vogt (GRV) leading-order quark distributions (82) with discarded flavor asymmetry of the sea, and it reads

$$f_u^{\text{val}}(y,t) = 1.239 y^{-\alpha_v - \alpha_v' (1-y)^{1/2} t}(1 - 1.8\sqrt{y} + 9.5y)(1-y)^{2.72}, \quad 89.$$

$$f_d^{\text{val}}(y,t) = 0.761 y^{-\alpha_v}(2y^{-\alpha_v'(1-y)^{1/2}t} - y^{-\beta_v'(1-y)t})(1 - 1.8\sqrt{y} + 9.5y)(1-y)^{3.62},$$

$$\bar{f}_u(y,t) = \bar{f}_d(y,t) = 0.76 y^{-\alpha_s - \alpha_s'(1-y)^{3/2}t}(1 - 3.6\sqrt{y} + 7.8y)(1-y)^{9.1}.$$

These models naturally reduce to the quark form factors with the dipole parameterization of proton and neutron Sachs form factors. The valence d-quark function has a more complicated structure, since the corresponding form factor F_1^d has a node at $|t| \approx 4M^2/|2\kappa_n + \kappa_p + 1|$: It is positive below this value and is negative above it. The Regge intercepts and slope parameters are taken as

$$\alpha_v = 0.52, \qquad \alpha_v' = 1.1\,\mathrm{GeV}^{-2}, \qquad \beta_v' = 1.0\,\mathrm{GeV}^{-2}, \qquad 90.$$
$$\alpha_s = 0.85, \qquad \alpha_s' = 0.3\,\mathrm{GeV}^{-2}.$$

The Regge parameters of the valence quarks are numerically close to those of ρ-reggeons, and the sea quarks being generated by gluon radiation are analogous to that of the pomeron. The form factor asymptotics at large t is governed by the large-y behavior of $f(y,t)$. If the latter has the form $f(y,t) \sim y^{-\alpha-\alpha'(1-y)^p t}(1-y)^N$, then the corresponding form factor is $F(t \to \infty) \sim |t|^{-(N+1)/(p+1)}$. The pQCD asymptotics for valence quarks requires $p = 1$. However, $p = 1/2$ is used for them because this value better fits the form factor at small and moderate t. For $p = 1$, one can get decent behavior at moderate t with $\alpha_u' = 1.6\,\mathrm{GeV}^2$. The estimates $b_{\mathrm{val}} = b_{\mathrm{sea}} = 1$ are used here. The D-term is parameterized as

$$D(z,t) = \left(1 - \frac{t}{m_{\mathrm{D}}^2}\right)^{-3} (1-z^2)(d_0\, C_1^{3/2}(z) + \cdots), \qquad 91.$$

with the mass scale $m_{\mathrm{D}}^2 = 0.6\,\mathrm{GeV}^2$ and the parameter d_0 computed within the chiral quark soliton model (χQSM) (4, 76) and on the lattice (73, 74). The results are as follows:

$$d_0^{\chi\mathrm{QSM}} = -4.0\frac{1}{N_f}, \qquad d_0^{\mathrm{latt}} = d_0^u \approx d_0^d \approx -0.5, \qquad 92.$$

respectively, where N_f is the number of active flavors. In the lattice case, the effect of disconnected diagrams was not calculated, but they are known to produce a sizable negative contribution (72). Once they are properly taken into account, the lattice result might approach the model calculation. For the present estimate an intermediate value, $d_0 = -1.0$, is chosen.

According to Section 3, the phase-space charge distribution $\rho_+(\vec{r}, x)$ is simply the Fourier transformation of the GPD,

$$\rho_+^q(\vec{r}, x) = \int \frac{d^3\vec{q}}{(2\pi)^3} \mathrm{e}^{-i\vec{q}\cdot\vec{r}} H^q(x,\xi,t), \qquad 93.$$

where $\xi = q_z/2E_q$, $E_q = \sqrt{M^2 + \vec{q}^2/4}$, and $t = \vec{q}^2$. Let us now consider the result of the quark densities from the above parameterization.

Figures 1 and 5 show the up-quark charge distributions calculated from $H_u(x,\xi,t)$ for various values of $x = \{0.01, 0.4, 0.7\}$. The intensity of the plots indicates the magnitude of the positive distribution; the lighter areas below the ground-zero contours indicate negative values. The plots show significant change in the distribution on the longitudinal momentum fraction x. The image is rotationally

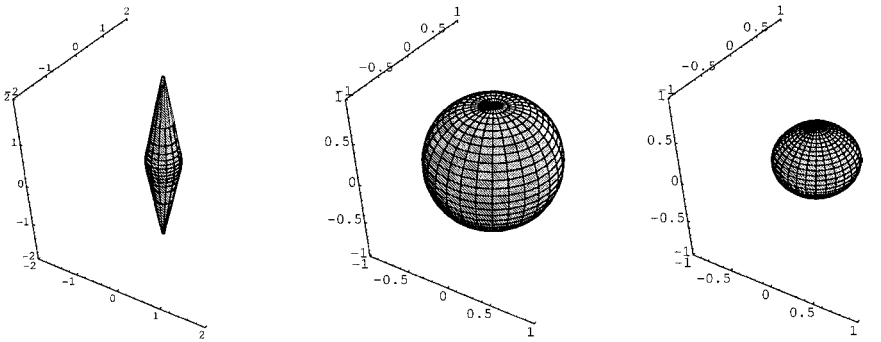

Figure 5 The u-quark phase-space charge distribution at different values of the Feynman momentum for a nonfactorizable parameterization of $H(x, \xi, t)$. Shown here are the shapes of three-dimensional isodensity contours ($\rho = \text{const}$) at $x = 0.01, 0.4$, and 0.7.

symmetric in the $\vec{r}_\perp$-plane. At small x, the distribution extends far beyond the nominal nucleon size along the z direction. The physical explanation for this is that the position-space uncertainty of the quarks is large when x is small, and therefore the quarks are delocalized along the longitudinal direction. This delocalization reflects a very peculiar part of the nucleon wave function and shows long-range correlations as verified in high-energy scattering. In a nucleus, the parton distributions at small x are strongly modified because of the spatial overlap between the nucleons. However, at larger x, the momentum along the z direction is of order nucleon mass, and the quarks are localized to within $1/M_N$. The quantum mechanical nature of the distribution becomes distinct because there are significant changes in the sign in different spatial regions.

6. SUMMARY

This article is an introduction to quantum phase-space parton distributions and generalized parton distributions. These novel distributions are important because of the deficiencies of the traditional nucleon observables—elastic form factors and Feynman parton distributions—neither of which contain any position or momentum space correlations. The new distributions encode precisely this information.

The new distributions are obtained by generalizing the concept of the Wigner distribution to relativistic quarks (and gluons) in QCD. Although the theoretical construction is by no means unique, one finds a class of six-dimensional distributions relevant for high-energy experiments. When integrating over the spatial coordinates, one has TMD (transverse-momentum-dependent) parton distributions. When integrating over the transverse momentum, one arrives at four-dimensional phase-space distributions. Fourier transformation of these distributions leads to GPDs.

This review has discussed several interesting properties of GPDs, including their connection to the quark orbital angular momentum and the spin structure of the nucleon. GPDs can be measured experimentally through hard-exclusive processes such as DVCS (deeply virtual Compton scattering). I presented a model GPD that satisfies a number of known constraints and provides a new and interesting visualization of the quarks in the quantum phase-space.

In the future, the most important goal in this field is to find ways to learn about these distributions. In addition to new experimental facilities and technology, lattice field theory will be an important complementary approach. Of course, any new theoretical method that helps to understand bound states in QCD will have a significant impact on our knowledge of the new distributions.

ACKNOWLEDGMENTS

I thank A. Belitsky, J.W. Chen, P. Hoodbhoy, J.P. Ma, and F. Yuan for collaborations, and M. Burkardt and T. Cohen for a number of helpful discussions. This work was supported by the U.S. Department of Energy via grant DE-FG02-93ER-40762.

The *Annual Review of Nuclear and Particle Science* is online at http://nucl.annualreviews.org

LITERATURE CITED

1. Belitsky A, Ji X, Yuan F. *Phys. Rev. D* 69:074014 (2004)
2. Diehl M. *Phys. Rep.* 388:41 (2003)
3. Ji X. *J. Phys. G* 24:1181 (1998)
4. Goeke K, Polyakov MV, Vanderhaeghen M. *Prog. Part. Nucl. Phys.* 47:401 (2001)
5. Radyushkin AV. In *At the Frontier of Particle Physics*, ed. M Shifman, 2:1037. Singapore: World Sci. (2001)
6. Ernst EJ, Sachs RG, Wali CK. *Phys. Rev.* 119:1105 (1960); Sachs RG. *Phys. Rev.* 126:2256 (1962)
7. Feynman RP. *Photon-Hadron Interactions.* New York: Benjamin (1972)
8. Wigner EP. *Phys. Rev.* 40:749 (1932)
9. Balasz N, Jennings B. *Phys. Rep.* 104:347 (1984); Hillery M, O'Connell RF, Scully MO, Wigner EP. *Phys. Rep.* 106:121 (1984); Lee HW. *Phys. Rep.* 259:147 (1995)
10. Vogel K, Risken H. *Phys. Rev. A* 40:2847 (1989)
11. Smithey DT, Beck M, Raymer MG, Faridani A. *Phys. Rev. Lett.* 70:1244 (1993); Breitenbach G, Schiller S, Mlynek J. *Nature* 387:471 (1997)
12. Banaszek K, Radzewicz C, Wodkiewicz K, Krasiński JS. *Phys. Rev. A* 60:674 (1999)
13. Dittes FM, et al. *Phys. Lett.* 209:325 (1988); Müller D, et al. *Fortschr. Phys.* 42:101 (1994)
14. Ji X. *Phys. Rev. Lett.* 78:610 (1997)
15. Burkardt M. *Phys. Rev. D* 62:071503 (2000)
16. Gao HY. *Int. J. Mod. Phys. E* 12:1 (2003)
17. Yennie D, Ravenhall M, Levy M. *Rev. Mod. Phys.* 29:144 (1957)
18. Brodsky SJ, Pauli H-C, Pinsky SS. *Phys. Rep.* 301:299 (1998); Burkardt M. *Adv. Nucl. Phys.* 23:1 (1996)
19. Ji X, McKeown R. *Phys. Lett.* B236:130 (1990)
20. Dragt A, Habib S. In *Quantum Aspects of Beam Physics*, ed. P Chen, p. 651. Singapore: World Sci. (1998)

21. Groenewold HJ. *Physica* 12:405 (1946)
22. Cohen L. *J. Math. Phys.* 7:781 (1966)
23. Husimi K. *Proc. Phys. Math. Soc. Jpn.* 22:264 (1940); Kirkwood JG. *Phys. Rev.* 44:31 (1933)
24. Ji X. *Phys. Rev. Lett.* 91:062001 (2003)
25. Efremov AV, Radyushkin AV. *Theor. Math. Phys.* 44:774 (1981)
26. Labastida JMF, Sterman G. *Nucl. Phys. B* 254:425 (1985)
27. Belitsky AV, Ji X, Yuan F. *Nucl. Phys. B* 656:165 (2003)
28. Sivers S. *Phys. Rev. D* 41:83 (1990); 43:261 (1991)
29. Brodsky SJ, Hwang DS, Schmidt I. *Phys. Lett.* B530:99 (2002)
30. Collins JC. *Phys. Lett.* B536:43 (2002)
31. Mulders PJ, Tangerman RD. *Nucl. Phys. B* 461:197 (1996)
32. Boer D, Mulders PJ. *Phys. Rev. D* 57:5780 (1998)
33. Boer D, Mulders PJ, Pijlman F. *Nucl. Phys. B* 667:201 (2003)
34. Ji X, Yuan F. *Phys. Lett.* B543:66 (2002)
35. Collins JC. *Acta Phys. Polon. B* 34:3103 (2003)
36. Hoodbhoy P, Ji X. *Phys. Rev. D* 58:054006 (1998)
37. Diehl M. *Eur. Phys. J. C* 19:485 (2001)
38. Soper DE. *Phys. Rev. D* 15:1141 (1977)
39. Ralston JP, Pire B. *Phys. Rev. D* 66: 111501 (2002)
40. Diehl M. *Eur. Phys. J. C* 25:223 (2002)
41. Belitsky AV, Müller D. *Nucl. Phys. A* 711:118 (2002)
42. Ashman J, et al. *Phys. Lett.* B206:364 (1988); *Nucl. Phys. B* 328:1 (1989)
43. Filippone B, Ji X. *Adv. Nucl. Phys.* 26:1 (2001)
44. Bernard V, Kaiser N, Meissner U-G. *Int. J. Mod. Phys. E* 4:193 (1995)
45. Chen JW, Ji X. *Phys. Rev. Lett.* 88:052003 (2002)
46. Belitsky A, Ji X. *Phys. Lett.* B538:289 (2002)
47. Gribov VN, Lipatov LN. *Sov. J. Nucl. Phys.* 15:138 (1972); Dokshitzer YuL. *JETP* 16:161 (1977); Altarelli G, Parisi G. *Nucl. Phys. B* 126:298 (1977)
48. Efremov AV, Radyushkin AV. JINR-E2-11535, Dubna (1978); Efremov AV, Radyushkin AV. *Phys. Lett.* B94:245 (1980)
49. Brodsky SJ, Lepage GP. *Phys. Rev. D* 22: 2157 (1980)
50. Belitsky AV, Müller D. *Phys. Lett.* B417:129 (1998); *Nucl. Phys. B* 537:397 (1999)
51. Martin AD, Ryskin MG. *Phys. Rev. D* 57: 6692 (1998)
52. Poblytsa PV. *Phys. Rev. D* 65:077504 (2002); *Phys. Rev. D* 65:114015 (2002); *Phys. Rev. D* 67:094012
53. Diehl M, Feldmann T, Jakob R, Kroll P. *Nucl. Phys. B* 596:33 (2001); erratum. *Nucl. Phys. B* 605:647 (2001)
54. Yuan F. *Phys. Rev. D* 69:051501 (2004)
55. Burkardt M. hep-ph/0401159
56. Vogt C. *Phys. Rev. D* 64:057501 (2001)
57. Hoodbhoy P, Ji X, Yuan F. *Phys. Rev. Lett.* 92:012003 (2004)
58. Braun V, Fries RJ, Mahnke N, Stein E. *Nucl. Phys. B* 589:381 (2000)
59. Chernyak VL, Zhitnitsky IR. *Nucl. Phys. B* 246:52 (1984)
60. Stefanis NG. *Eur. Phys. J. C* 1:7 (1999); Gari M, Stefanis NG. *Phys. Rev. D* 35: 1074 (1987)
61. Ji CR, Sill AF, Lombard RM. *Phys. Rev. D* 36:165 (1987)
62. Ji X. *Phys. Rev. D* 55:7114 (1997)
63. Belitsky AV, Müller D, Niedermeier D, Schäfer A. *Nucl. Phys. B* 593:389 (2001)
64. Belitsky AV, Müller D, Kirchner A. *Nucl. Phys. B* 629:323 (2002)
65. Guidal M, Vanderhaeghen M. *Phys. Rev. Lett.* 90:012001 (2003)
66. Belitsky AV, Muller D. *Phys. Rev. Lett.* 90:022001 (2003); *Phys. Rev. D* 68: 116005 (2003)
67. Airapetian A, et al. *Phys. Rev. Lett.* 87:182001 (2001); Stepanyan S, et al. *Phys. Rev. Lett.* 87:182002 (2001); Adloff

C, et al. *Phys. Lett.* B517:47 (2001); Saull FR, et al. hep-ex/0003030
68. Brodsky SJ, et al. *Phys. Rev. D* 50:3134 (1994)
69. Radyushkin AV. *Phys. Lett.* B385:333 (1996)
70. Collins JC, Frankfurt L, Strikman M. *Phys. Rev. D* 56:2982 (1997)
71. Mathur N, et al. *Phys. Rev. D* 62:114504 (2000)
72. Gadiyak V, Ji X, Jung C. *Phys. Rev. D* 65:094510 (2002)
73. Göckeler M, et al. hep-ph/0304249
74. Hägler P, et al. *Phys. Rev. D* 68:034505, 2003
75. Ji X, Melnitchouk W, Song X. *Phys. Rev. D* 56:5511 (1997)
76. Petrov VY, et al. *Phys. Rev. D* 57:4325 (1998)
77. Polyakov MV, Weiss C. *Phys. Rev. D* 60: 114017 (1999)
78. Boffi S, Pasquini B, Traini M. *Nucl. Phys. B* 649:243 (2003); Schweitzer P, Boffi S, Radici M. *Phys. Rev. D* 66:114004 (2002); Scopetta S, Vento V. *Eur. Phys. J. A* 16:527 (2003)
79. Radyushkin AV. *Phys. Rev. D* 56:5524 (1997)
80. Radyushkin AV. *Phys. Lett.* B449:81 (1999)
81. Burkardt M. *Int. J. Mod. Phys. A* 18:173 (2003)
82. Gluck M, Reya E, Vogt A. *Eur. Phys. J. C* 5:461 (1998)

Annual Review of Nuclear and Particle Science
Volume 54, 2004

CONTENTS